Peer-reviewed version available at *Sustainability* **2018**, *10*, 3953; doi:10.3390/su10113953

Article

Agro-economic Water Productivity-based Hydro-economic Modeling for Optimal Irrigation and Crop Pattern Planning in the Zarrine River Basin, Iran, in the Wake of Climate Change.

Farzad Emami [1], and Manfred Koch[1]*

[1] Department of Geohydraulics and Engineering Hydrology, University of Kassel, 34125 Kassel, Germany

* Correspondence: farzad.emami@student.uni-kassel.de; Tel.: +17672702711

Abstract: For water-stressed regions like Iran, improving the effectiveness and productivity of agricultural water-use is of utmost importance due to climate change and unsustainable water demands. Therefore, a hydro-economic model has been developed here for the Zarrine River Basin with the central concept of that demands are value-sensitive functions, where quantities of water-uses at different locations and times have a changeable economic benefits. To do this, the surface and groundwater resources changes, especially the Boukan Dam, and the potential crop yields are simulated using the hydrologic model, SWAT, based on the GCM/QM-downscaled climate predictions. Then, a basin-wide water management tool, MODSIM, is customized to allocate the agricultural water based on the agro-economic water productivity (AEWP) of crops. Next, a coupled CSPSO-MODSIM hydro-economic model has been developed via a simulation-optimization approach, to optimize the total AEWP, considering climatic impact and crop pattern scenarios for three future periods: 2020-2038, 2050-2068 and 2080-2098. Finally, the optimal crop pattern and crop water irrigation depths are presented for different RCPs and periods. The results indicated that this method will improve considerably the AEWPs and decrease the agricultural water-use by near 40%. Thus, this integrated model is able to support water authorities and other stakeholder in a water-scarce basin, as is the study area.

Keywords: Agro-economic water productivity; Hydro-economic modeling; CSPSO-MODSIM; Economic benefits; Optimal crop pattern; Optimal crop water irrigation depth; Climate change; Iran.

1. Introduction

Food and water security will pose a great challenge in the near future due to rapid growth of population and often unsustainable water usage. The renewable water resources per capita in the Middle East and North Africa (MENA), as the most water- scarce regions of the world, are expected to decline from 750 to 500 m³ by 2025, while the water withdrawals will increase by up to 50% [1].

Natural and anthropogenically induced climate change will act as an additional external driver threatening the future food security by exacerbating the water shortage and, concomitantly, the decrease of crop production, as temperatures and irrigation water requirements increase [2]. All this holds particularly for the Middle East, including Iran, where groundwater reserves diminish at an alarming rate [3].

Improving the efficiency of agricultural water use is of utmost importance, as irrigation water uses account for 70% of the global freshwater withdrawals, particularly due to the fact that the irrigated areas have dramatically increased in the 20th century, providing now about 40% of the world's food [4,5]. In addition, agriculture has also an important role in the economy, in terms of the

Preprints (www.preprints.org) | NOT PEER-REVIEWED | Posted: 20 August 2018 doi:10.20944/preprints201808.0361.v1

Peer-reviewed version available at Sustainability 2018, 10, 3953; doi:10.3390/su10113953

Global Gross Domestic Product (GDP), especially, in developing countries, although its share has been decreasing over the last twenty years [6]. Thus for Iran the GDP contribution of agriculture decreased from 23 to 9 % [7], although the irrigated lands increased by 17% between 2003 and 2008 [8] and 90% of the food demands are derived from agriculture supplies in Iran, but with a cost of exploitation of 92% of the available freshwater resources [5] which indicates that the economic return on water use is outstandingly low in Iran.

The agricultural production will also need to be increased globally by 70% up to year 2050, due to a 40%- projected population increase [9]. The situation is even worse for developing countries where the food production should be doubled by that time [10]. Such a global production growth can, to 90%, only be achieved by agricultural land expansions instead of crop yield enhancements [4].

For a long-term sustainable water resources management for agriculture it is important to quantify and evaluate the possible impacts of climate change scenarios on the future water availability and crop production potentials. Previous publications evaluated the impacts of climate change on the water resources using hydrologic simulation models based on GCM- predictions [11,12]. These and numerous other studies indicate that climate change will have undeniable impacts on the hydrology, namely, streamflow changes in a basin, which ultimately affects the water availability there.

For example, the impacts of climate change on the crop yield, food security and crop water demands in sub-Saharan Africa and the North China Plain are investigated by Chijioke et al. and Mo et al. [13,2], respectively, using different crop prediction and simulation models. These studies show that climate change may have either beneficial or harmful effects on the crop extent and productivity in irrigated or rain-fed agricultural lands. Other recent studies focus on the analyses of the impacts of a changing climate and agricultural demands on the water management and crop production [14,15] and indicate that climate change will lead to hydrologic changes and thus alter crop yields and crop water productivity (CWP), so that some adaptation strategies are required.

Over recent years many publications on optimizing crop pattern and water allocation to maximize crop productions and economic benefits and to enhance the agricultural water management have appeared. A multi-crop planning (MCP) optimization model based on a nonlinear programming (NLP) algorithm was utilized for cropping pattern and water allocation by Bou-Fakhreddine et al. [16]. Firstly, two linear formulations and a relaxed version were established from the NLP and then the MCP problem is solved by implementing two meta-heuristic algorithms, Simulated Annealing (SA) and Particle Swarm Optimization (PSO). Fazlali and Shourian [17] optimized water allocation by considering optimum cropping pattern for the Arayez plain in Iran, using the Shuffled Frog Leaping Algorithm coupled with MODSIM [18] and employing irrigations depths and cultivation areas as decision variables. However, the authors did not consider the CWP index, impacts of climate change and management of the conjunctive water uses. In fact, few of these issues have been addressed by Fereidoon and Koch [19] who employed a MODSIM-LINGO-PSO algorithm to maximize the economic benefits of the Karkheh Dam in Iran, in terms of water allocation for agriculture, under the impact of future climate change. The authors separated the optimization into a three-stage procedure, wherefore in the first step the MODSIM allocates the available water of Karkheh Dam, with its inflow simulated by the SWAT-hydrological model. Then, a linear optimization to maximize the crop yields in response to different assumed levels of available water is carried out and, finally, a PSO algorithm is used to maximize the economic agricultural benefits.

The purpose of the current research is to jointly optimize the crop pattern and irrigation planning under climate change- and cropping pattern scenarios and so to maximize the net economic return and total CWP altogether. This objective is achieved by using an integrated hydro- economic model which consists of a combination of the CSPSO (Constrained Stretched Particle Swarm Optimization) method and MODSIM water management and planning model as a simulation- optimization approach.

The research area is the Zarrine River Basin (ZRB) belonging to the basin of Lake Urmia (LU), which has been shrinking tremendously over the recent decades. The impacts of climate change scenarios on the water resources and the crop production will be evaluated considering the crop

Preprints (www.preprints.org) | NOT PEER-REVIEWED | Posted: 20 August 2018 doi:10.20944/preprints201808.0361.v1

Peer-reviewed version available at *Sustainability* **2018**, *10*, 3953; doi:10.3390/su10113953

pattern scenarios for the irrigated croplands using the available water supply sources, namely, the Boukan Dam as the most important water management infrastructure of the region, as well as inter-basin discharges from river reaches and groundwater shallow aquifers.

To simulate the basin's water resources, i.e. the inflow of the Boukan Reservoir, interbasin flows, groundwater recharges and other hydrologic variables of the ZRB in response to the changing climate, future (up to year 2098) downscaled climate predictors (min. and max. temperatures, precipitation) are taken from the recent study of Emami and Koch [12], and entered into the river basin hydrologic model, SWAT which is firstly calibrated and validated for the discharge and then for the crop yields by adjusting the crop parameters and crop water requirements. Next a water planning and management simulation model is prepared, using MODSIM for managing the conjunctive agricultural water uses in the river basin. The model is customized to allocate the available water to the major crop arable areas of the ZRB based on the crop water productivity (CWP) and the net economic benefit (NEB) of the crop production, both of which are combined in an index of agro-economic water productivity (AEWP). Finally, to enhance the crop production and efficiency of the water management policy, a Constrained Stretched Particle Swarm Optimization (CSPSO) algorithm is developed and fully coupled with the MODSIM model in order to maximize the total AEWP of the ZRB, as the objective function. The optimal arable crop areas and corresponding irrigation schedules are determined using this CSPSO-MODSIM model under the constraints of arable areas for the irrigation plots and three different cereal crop pattern scenarios considering three impact scenarios of climate change (RCP45, 60 and 85) for three future periods (near, middle and far).

2. Study region and data

2.1. The Zarrine River Basin

The Zarrine River is the main inflow source of the LU, the largest inland wetland of Iran which used to be the largest lake in the Middle East before it dwindled significantly in recent decades, with detrimental effects on the surrounding ecosystems of the lake. The Zarrine River Basin (ZRB) is located in northwestern Iran, south of LU between 45°46′ E to 47°23′ W longitude and 35°41′ S to 37°44′ N latitude (see Figure 1). The total length of the main channel is about 300 km and most of its course stretches through a mountainous area. The basin covers an area of about 12,000 km^2 including parts of Kurdestan and the West and East Azarbaijan provinces, wherefore its larger portion is mountainous with an elevation of up to 3297 m and the smaller one is rather plain with an elevation going down to 1264 m. The big cities of the basin are namely Miandoab, Shahindej, Tekab and Saghez.

The climate of the region varies from semi-wet cold or wet-cold in the mountain areas to semi-dry in the vicinity of LU. The average annual temperature varies between 8 and 12 °C while the annual precipitation (rain and snow) in the basin varies between 200 mm/yr in the lower catchment area and 800 mm/yr in the mountains. The maximum snowfall is recorded mostly in the south and west of the basin with snow heights varying from 5 to 63 mm/yr.

The Boukan Dam/Reservoir is the largest operating dam of the ZRB, with a gross storage capacity of 760 million m^3 (MCM) and a live storage capacity of 654 MCM. Its water is used for agricultural irrigation and the supply of drinking water (110 MCM/yr).

The agricultural areas within the basin cover a total area of 74,318 ha, all irrigated by both groundwater and surface water resources, including water from the Boukan Reservoir, as the crop-growing season there is mostly during the dry months between spring and autumn.

The current applied irrigation efficiency is about 38% for the areas irrigated by the surface water resources from the dam and the river, and 50% for the areas using groundwater resources; all numbers which are lower than the averages of most developing countries (45%) and developed countries (60%) [20]. indicating a non-efficient use of surface water due to outdated irrigation methods and systems with a large loss of water.

It should also be noted that the area of irrigated land has been increased by 36% between 1976 and 2013 [21], and this in spite of a catastrophic 88%- decrease of the LU surface and ensuing environmental and ecological crises.

Preprints (www.preprints.org) | NOT PEER-REVIEWED | Posted: 20 August 2018 doi:10.20944/preprints201808.0361.v1

Peer-reviewed version available at *Sustainability* **2018**, *10*, 3953; doi:10.3390/su10113953

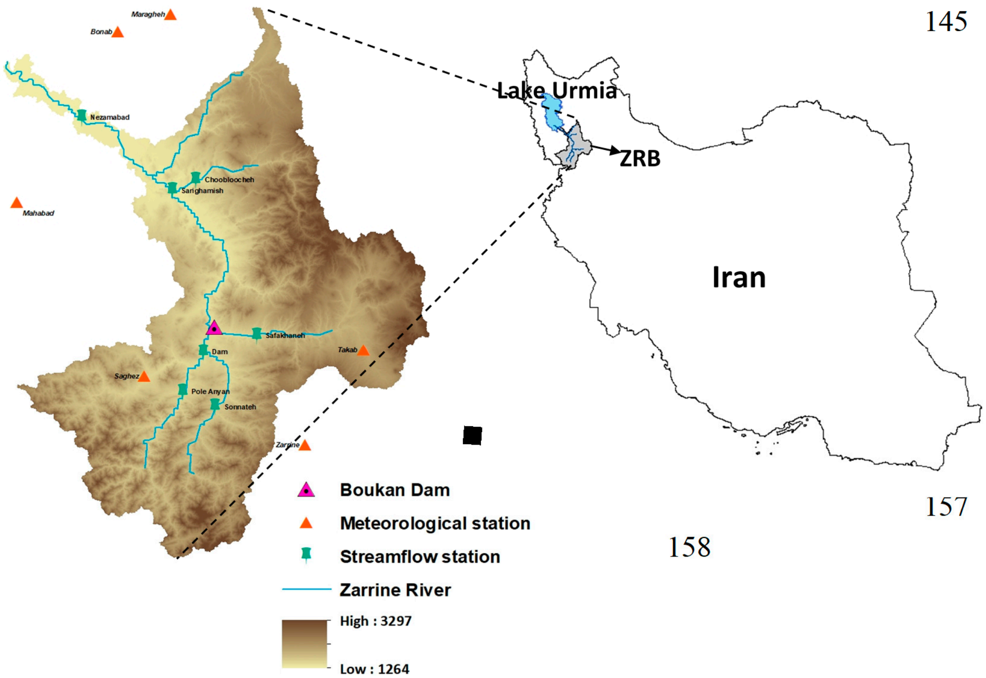

Figure 1. Map of the ZRB with Boukan Dam and weather and streamflow stations.

The irrigated croplands of the ZR Basin are demonstrated in Figure 2, including the current irrigated croplands of the ZRB (green) and the future agricultural development plan of ZRB namely Rahimkhan (RK) Plain (light green) located in the downstream of the Boukan Dam. The main agricultural crops of the ZRB as well as the RK include alfalfa (ALFA), apple (APPL), barley (BARL), potatoes (POTA), sugar beet (SGBT), tomatoes (TOMA), wheat (WWHT) and these are the ones are considered in this study.

2.2. Data

The data needed for this study in the ZRB is gathered from different available sources. Most of the data is required for the set-up of the SWAT- hydrologic model, namely, various geospatial maps and hydro-climate time series.

The Digital Elevation Map (DEM) with a spatial resolution of 85 m was produced by the Iranian surveying organization. The land-use classification map of the basin, demonstrating the situation in year 2007, was obtained from the Agricultural Statistics and the Information Center of the Ministry of Agriculture [22] and has a resolution of 1000 m and distinguishes 10 land use classes. The soil map of the watershed was extracted from the Food and Agriculture Organization (FAO) digital soil global map, with a spatial resolution of 10 km of and 8 types of soils within two layers.

The climate input data includes daily maximum and minimum temperatures and daily precipitation over the period of 1987 to 2015 and was obtained from the Iranian Meteorological Organization (IRIMO) for six synoptic stations located in or close to the ZRB (see Figure 1). Missing data in the records were filled in using the inverse distance weighting (IDW) interpolation method. As the daily data for other climate variables, including solar radiation, wind and relative humidity, were unavailable, they were generated using the weather generator (WGEN) module of the SWAT model based on monthly averages of the synoptic stations of Iran.

Daily streamflow data for six gauging stations of the Zarrine River (Figure 1) were obtained from the Iran Ministry of Energy for the period 1987 to 2012.

The crop and irrigation data, namely, crop irrigation sources, planting, irrigation and harvesting dates or water demands were taken from Ahmadzadeh et al. and MOE [23,24]. The observed crop yields are gathered from MOA [22] and the additional economic crop data were gathered from SCI and MOA [25,26].

Peer-reviewed version available at *Sustainability* **2018**, *10*, 3953; doi:10.3390/su10113953

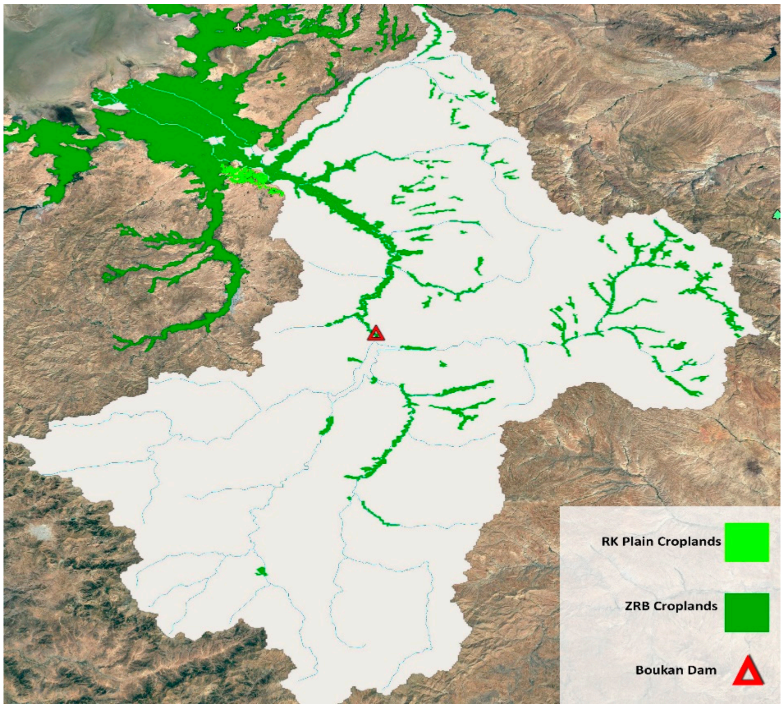

Figure 2. Locations of irrigated croplands of the ZRB and the RK plain and the Boukan Dam.

3. Methodology: Development of an integrated hydro- economic model for optimal water management and crop pattern

3.1. Basic concepts of an optimal hydro- economic model

Generally the greater the water-use efficiency and productivity, the lower are the conflicts over scarce water resources and the additional financial and environmental burdens in an agriculturally exploited basin like the ZRB. Enters the fundamental concept of hydro-economics which stipulates that water demands can be represented as value-sensitive water demand functions, so that water-uses at different locations and times have varying economic benefits [27]. The next step is then to set up a hydro-economic model, which is a solution-oriented model for investigating the water management tradeoffs and improving the efficiency of water allocation by incorporating the economic value of agricultural water in the heart of the water management model. This model represents a spatially distributed water resources system, infrastructure, management options and economic values comprehensively [27]. In the third and final step such a hydro-economic model may be applied to simulate agricultural crop pattern strategies, with the goal to find that optimal multi-crop pattern which somehow maximizes the economic crop profits, while adhering to the various constraints of the limited water resources, hydrology, and various environmental regulations. Mathematically, this amounts to the set-up of a classical constrained (nonlinear) optimization problem, wherefore (1) the forward problem, i.e. the objective or cost function, is computed by the hydro-economic model, simulating the hydrological constraints by classical hydrological models, and (2) the minimization of that objective function is done by some kind of an optimization routine (e.g. [19]).

In this section an innovative hydro-economic model for the ZRB is developed using such a simulation-based optimization approach to coordinate multiple factors including water allocation, crop production pattern and economic gains. More specifically, the optimization problem is defined as a constrained optimization (CO) problem which searches for the optimal allocation of irrigated crop pattern under the constraints of the limited water resources and other demands that should be satisfied. Eventually, the objective of the optimization search algorithm is to maximize the agro-economic productivity, i.e. the economic net benefit of a crop per unit water use, given that the latter

Preprints (www.preprints.org) | NOT PEER-REVIEWED | Posted: 20 August 2018 doi:10.20944/preprints201808.0361.v1

Peer-reviewed version available at Sustainability 2018, 10, 3953; doi:10.3390/su10113953

is limited in the study region and may be even more so in the future under the impacts of imminent climate change there [12].

The decision variables of the optimization are the cultivated areas of the major crops for a particular, politically given combination of required crop distribution and agricultural demand regions. The constraints of the optimization algorithm in this study are defined based on the allowable range of arable areas and the cereal crop pattern limits. More details are provided in Section 3.6.

3.2. *Modules of the CSPSO-MODSIM integrated hydro- economic model*

The individual modules (hydrological, water management, agro-economic) of the hydro-economic model are developed in this research using different simulation models (GCM, QM, SWAT, MODSIM) bound together with an optimization method (CSPSO). The flow chart of the connection of the models and processes in the integrated hydro-economic model is presented in Figure 4, from which the main steps are retrieved as follows:

- Predicting climate change weather scenarios using CMIP5-GCMs predictors that are subsequently downscaling by QM.
- Simulating the future hydrologic changes and crop yields with the calibrated SWAT river basin hydrological model using the QM climate projections as input drivers.
- Setting up a basin-wide water management and planning module, MODSIM, to allocate the future agricultural water uses efficiently based on the initial agro-economic productivity of the crops.
- Optimizing the crop arable areas and the related irrigation schedule using the agro-economic water productivity- based hydro-economic model, CSPSO-MODSIM.

Details of each of the above modeling steps are described in the following sub-sections.

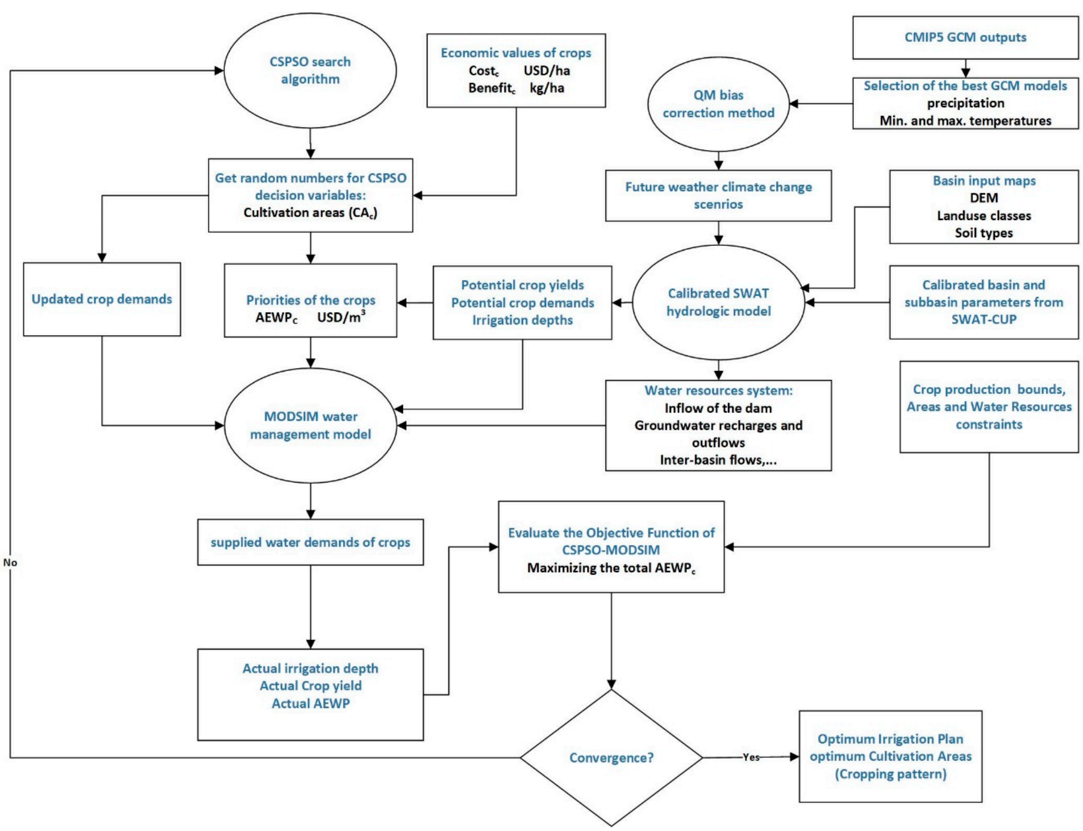

Figure 3. Flowchart of the CSPSO-MODSIM hydro-economic optimization model.

Peer-reviewed version available at Sustainability 2018, 10, 3953; doi:10.3390/su10113953

3.3. Predicting future climatic scenarios by updated quantile mapping

Regarding the projections of future climate change scenarios, they are mostly taken from Emami and Koch [12] who used several climate models (GCMs) of the CMIP5 archive [28] as mentioned in the fifth IPCC report [29] to select the most suitable one based on a climate model's skill to simulate the past climate in terms of minimum and maximum temperatures and precipitation. For assessing the impacts of climate change on the regional scale, the climate predictors of the selected GCM models were then downscaled using a recently-coming-to-the-fore statistical downscaling method, namely, QM (Quantile Mapping) [30,31], which proved to have better prediction performances than the more commonly used classical statistical downscaling model (SDSM). We forego a detailed description of the QM-downscaling method and refer the reader to [12].

In the first step of the QM method, the monthly biases of the future GCM- simulated climate variables between year 2020 to 2098 are removed using a trend-preserving bias correction, namely, ISI-MIP approach [30]. In this approach the GCM- simulated temperatures (min. and max.) are corrected applying an additive correction factor CT_j and for the precipitation and a multiplicative correction factor CP_j to each month of a year (j=1,..12) of the GCM-simulated precipitation. In the second step a new, updated quantile mapping method [31] is used to correct the daily biases of the temperatures and precipitation in each month (e.g. all Januaries) using EDCDFm and CNCDFm CDF- (cumulative distribution function) matching methods, respectively. Emami and Koch [12] proved that these QM-variants perform better than other statistical downscaling methods in removing biases in the GCM- climate predictors for the study region by delivering much better correlations with the observed predictands (temperatures and precipitation) at the high-resolution, local scale, and all this without almost no extra computational costs.

3.4. SWAT- simulation of the hydrological processes in the agricultural watershed.

3.4.1. Model setup and calibration

The Soil Water Assessment Tool (SWAT) model is a physically-based, river basin-scale, time continuous simulation model that operates on a daily time step. Although this model has originally been developed to mainly simulate the impacts of land management practices in large and complex watersheds [32], it is widely used as a long-term rainfall-runoff model and efficient hydrologic simulator of water quantity and quality, so that it has increasingly being used to investigate climate change impacts on agro-hydrological systems [11,33].

The SWAT model requires quite a wide range of input data, as described in Section 2.2. To represent the large-scale spatial heterogeneity of the study basin more precisely, the SWAT modeled domain, i.e. the major basin, is divided into several sub-basins, usually delineated with the help of the topographic DEM using the ARCSWAT extension of ARCMap program. Then, each sub-basin is parameterized using a set of HRUs (Hydrologic Response Units) which are based on a unique combination of soil and land cover and management. For the SWAT-model of the ZRB, 11 sub-basins (as shown in Figure 1) with a total of 908 HRUs have been defined.

After the parameterization of the SWAT- model's input data entries is done by using the stochastic sequential uncertainty fitting version 2 (SUFI-2) optimization algorithm embedded in the SWAT-CUP decision-making framework [34]. Various kinds of objective functions as measures for the goodness of the fit of the modeled to the observed streamflow are available in the SUFI-2 algorithm, wherefore Krause et al. [35] indicates that for a reliable calibration and validation of the model a combination of different efficiency criteria, such as the coefficient of determination R^2 , the Nash–Sutcliff efficiency coefficient NSE, and bR^2 (b is the slope of the regression line between observed and simulated streamflow), should be considered.

In the present application the calibrated input parameters of the model have been taken from Emami and Koch [12], where further details of the calibration/ validation as well as the model setup

Preprints (www.preprints.org) | NOT PEER-REVIEWED | Posted: 20 August 2018 doi:10.20944/preprints201808.0361.v1

Peer-reviewed version available at Sustainability 2018, 10, 3953; doi:10.3390/su10113953

are presented. Basically, the optimal range of model input parameters was determined hierarchically sub-basin-wise, from the utmost upstream sub-basin (11) outlet down to the main outlet of the basin.

Based on the SUFI- sensitivity analysis, 24 model parameters were shown to be sensitive parameters for affecting the stream discharge, out of which the SCS curve number (*CN2*), the groundwater delay time (*GW_DELAY*) and the moist bulk density of the soil (*SOL_BD*) turned out to be the three most sensitive variables. With these optimized parameters good fits of the modeled to the observed discharges were obtained at the six streamflow stations (sub-basin outlets) for the calibration (1998- 2012) and the validation (1991-1997) periods, with average R^2> 0.7, *NSE*>0.6 and bR^2>0.5 which, according to the classification proposed by Moriasi et al. [36], is considered satisfactory. As the SUFI-computed uncertainty of the calibrated model which is quantified by the *P*- and the *R*-factor (see [37,12]) has average values of *R* >0.75 and *P* close to 1, there is enough confidence in the calibrated SWAT- model for the ZRB.

3.4.2. Predicting the impacts of future climate change on the hydrologic cycle

It is important to evaluate the hydrologic responses to future changes of climate for improving adaptive water management, as the variability of precipitation and temperature in terms of trends and extremes will eventually increase the likelihood of severe and irreversible negative impacts on the ecosystem including lakes and rivers. To that avail, the future downscaled climatic scenarios i.e. the QM- bias corrected predictions of the minimum and maximum temperatures and precipitation are employed as weather input drivers of the calibrated basin-wide hydrologic simulation model, SWAT. As a result, the future hydrologic cycle and the available water resources of the ZRB under the climate change can be assessed, especially the input of the dam, the Inter-basin discharge of the river reaches, the groundwater recharges and the withdrawals of the shallow aquifers.

3.4.3. Crop yield simulation and calibration of the potential crop yield

The SWAT model is also capable of simulating crop productions and yields efficiently, as has been shown in many publications (e.g. [38,39]). To do this in the ZRB, the current management operations of the various crops there are specified initially in the SWAT model, together with the corresponding planting and harvesting dates and the irrigation sources, based on information given by Ahmadzadeh et al. [24]. The crop yields for seven major crops in the ZRB are then calibrated by adjusting a set of effective parameters in the model, until the averages of the simulated crop yields of the basin match those of the observed ones (gathered from MOA [22]) in a reasonable manner. These simulated crop yields are then extracted from the SWAT file output.hru to represent the potential crop yields of the ZRB.

3.5. Water resources management and planning module

3.5.1. Agro-economic water productivity

For a better management of the future water resources in a water-scarce region, such as the ZRB, it is necessary to make the water supply- and/or the irrigation system as efficient as possible. Because of the competition of the different stakeholders for the scarce freshwater resources in the region, not only for agriculture, a paradigmatic policy shift is required from a) maximizing productivity per unit of area to b) maximizing productivity or economic value per unit of consumed water [40], as both the irrigated agriculture's land base and the water supplies are continuously being depleted and reallocated, in order to produce even more agricultural crops. To achieve this policy shift, the net benefits of the water used, i.e. the productivity per unit of water should be increased.

The crop-water productivity CWP_c (kg/m^3) is defined as the ratio of the amount of crop yield produced Y_c (kg/ha) to the amount of water delivered per unit crop area Q_c (m^3/ha) during the crop's production [41]. The next step is then to define the agro-economic water productivity $AEWP_c$ (USD/m^3) as the ratio of the net total economic value of the crop NEB_c (USD) to the total amount of water Q^t_c (m^3) delivered under the priority constraints provided by MODSIM (see following subsection) [42]:

$$AEWP_c = NEB_c \;/\; Q^t_c = [(Price_c * Y_c - Cost_c) * A_c] \;/\; Q^t_c = (Price_c * Y_c - Cost_c) \;/\; Irr_c \qquad (1)$$

where $Price_c$ (USD/kg) is the selling price of the crop, $Cost_c$ (USD/ha) is the total production costs of the crop, A_c (ha) is the crop cultivation area, $Irr_c = Q^t_c / A_c$ (m) is the irrigation water height, and the other variables are as defined above .

Based on the definitions above, for boosting the agro-economic water productivity $AEWP_c$ as the ultimate objective, it is firstly necessary to increase the crop water productivity CWP_c, particularly, in areas where the water is scarce. This can be achieved by adopting proven agronomic and water management practices, such as deficit irrigation or modern irrigation technologies (e.g. pressured systems and drip irrigation). Next, to improve the economic yield then one may need to (a) switch from low- to high-value crops, for example, from wheat to strawberry, (b) lower the costs of inputs (labor, water technologies), (c) attempt to get multiple benefits of the irrigation water, e.g. using (cheaper) recycled wastewater [42]. Eventually, it may be recommendable to replace water-thirsty, sensitive crops by more drought-resistant crops, e.g. Pistachio [43].

3.5.2. MODSIM water resources management model

The MODSIM simulation model is a generalized river basin network model for developing basin-wide strategies of short-term water management, long-term operational planning, drought contingency planning, water rights analysis and conflict resolution between different water users [18,44]. This model has enjoyed widespread application across the world to simulate operations as mentioned [45-47,19].

The core idea behind MODSIM is to represent a complex river basin system by a flow network consisting of coupled sequences of nodes and links, with the former symbolizing storage components, such as reservoirs and aquifers, points of inflow, demands, diversions, and river confluences, and the latter representing river reaches, pipelines, canals, and stream-aquifer interconnections defining stream depletions from pumping and return flows from seepage and other water applications. Further network elements of the model consist of unregulated inflows, reservoir operating targets, consumptive and instream flow demands, evaporation and channel losses, reservoir storage rights and exchanges, and stream-aquifer modeling components. In addition, various surface and ground water resources with their inter-relationships can be represented by highly nonlinear, non-convex or discontinuous equations [48]. Details on how each of the components is modeled and calculated in the model can be found in Fredericks et al. [18].

The model sequentially solves a linear optimization problem within the confines of mass balance throughout the network over the planning period by means of a highly efficient network flow optimization (NFO) algorithm solved with the Lagrangian relaxation algorithm RELAX-IV [49]. More specifically, the following constrained flow optimization problem is solved for each time interval (t=1,…,T) over the planning horizon:

$$\textit{Minimize} \qquad \sum_{k \in A} c_k q_k \qquad (2)$$

subject to:

$$\sum_{k \in O_i} q_k - \sum_{k \in O_i} q_k = b_{it}\,; \quad \textit{for all nodes } i \in N \qquad (3)$$

$$l_k \le q_k \le u_k\,; \textit{for all links } k \in A \qquad (4)$$

where A is the set of all links in the network; N is the set of all nodes; q_k is the integer valued flow rate in link k; c_k are cost weighting factors, i.e. the water right priorities per unit flow rate in link k; b_{it} is the (positive) gain or (negative) loss at node i at time t; I_i the set of all links terminating at node i (inflow links); O_i the set of all links originating at node i (outflow links); and l_k and u_k are lower and upper bounds, respectively.

The cost factor c_k for accounting for active storage and demand links priorities are generally calculated using the following formula:

$$c_k = -(50000 - 10 * PR_k) \qquad (5)$$

where PR_k is the integer priority ranking which ranges between 1 and 5000 for the reservoirs or the demands, where the negative sign states that high-rank nodes (1, 2, etc.) are given more weights in the minimization of the cost function (Eq. 2).

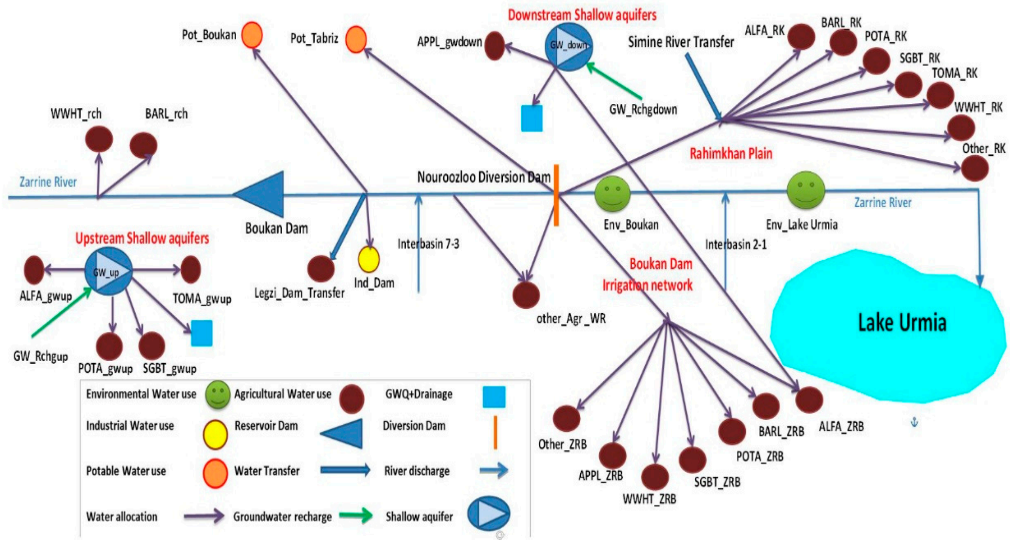

Figure 4. Schematics of the MODSIM model for the ZRB with related demand nodes, separated into three demand area groups as indicated by the corresponding suffixes.

The cost factor may also include economic factors which are defined in this study for the crop demand links as the cost of the crop water supply (cc_c) based on the agro-economic water productivity index $AEWP_c$ (Eq. 1), i.e. cc_c=-$AEWP_c$ which means that more water should be allocated to a crop that provides more economic benefits than others for the same amount of water delivered.

The schematic network of the MODSIM ZRB model with the various demand nodes represented in Figure 3. These demand nodes can be categorized into four groups: (1) the network of the dam croplands (ZRB), suffixed _ZRB, (2) the future development croplands of the RK, suffixed _RK, (3) the crop demands supplied from the reach, suffixed _rch, and (4) the demands supplied from the groundwater aquifers, wherefore two aquifer storages are defined cumulatively for the upstream-, suffixed _gwup, and downstream, suffixed gwdown areas of the Boukan dam. The conjunctive water uses, i.e. surface- and groundwater irrigation are linked by connecting the river network nodes and the shallow aquifer storages with the corresponding demand nodes. Other non-agricultural water demands include the potable demand of Boukan and Tabriz cities, the industrial demands of the dam, the Legzi water transfer, the other agricultural water rights, the environmental rights of the Boukan Dam and the LU environmental water demand.

The hydrologic inputs for the MODSIM- model are captured from the flow results of the SWAT model, including the inflow of the dam, the river discharges and the inter-basin flows (the inter-basins 7-3 and 2-1 describe the generated water in sub-basins 7 to 3 and sub-basins 2 to 1, respectively), the storage of the shallow aquifers, the recharges (GW_Rchg), the contributing flows to the surface water and the drainage (GWQ + Drainage). The different types of the water demands, water transfers (such as the transfer to the RK Plain from the Simineh River) are all initially defined based on values given by MOE [24] and the irrigation and water requirements of the various crops are adjusted based from provisional values of Ahmadzadeh et al. [23].

The MODSIM ZRB simulation model is customized on the MODSIM 8.5 platform using the custom coding module in VB.NET routine, with further details provided in Section 3.6.

3.6. Constrained Stretched Particle Swarm Optimization (CSPSO) search algorithm

The Particle Swarm Optimization (PSO) method proposed first by Kennedy and Eberhart [50] is a stochastic evolutionary social behavior-based optimization algorithm for solving nonlinear global optimization problems in an efficient way. The main idea behind the development of the PSO is social

Preprints (www.preprints.org) | NOT PEER-REVIEWED | Posted: 20 August 2018 doi:10.20944/preprints201808.0361.v1

Peer-reviewed version available at Sustainability 2018, 10, 3953; doi:10.3390/su10113953

sharing of information among individuals of a population in nature (the flock or swarm), in order to provide an evolutionary advantage for all individuals to move towards some optimum [51-53].

A PSO model consists of a number of N particles (the swarm) moving around in the D-dimensional search space, with each particle representing a possible solution to a numerical problem. In this D-dimensional search space the actual location of the i-th particle (i=1,…,N) can be represented by a D-dimensional vector of position $X_i = (x_{i1}, x_{i2}, \ldots, x_{iD})$ and the position change (velocity) by another D-dimensional vector $V_i = (v_{i1}, v_{i2}, \ldots, v_{iD})$. The best candidate solution which is the best previously visited position of the particles of the swarm is denoted as $P_i = (p_{i1}, p_{i2}, \ldots, p_{iD})$.

Assuming that the g-th particle is the best and denoting the iteration by the superscript n, the swarm is manipulated according to the following two equations [54,55]:

$$v_{id}^{n+1} = \chi\left(\omega^n v_{id}^n + c_1 r_1^n (p_{id}^n - x_{id}^n) + c_2 r_2^n \left(p_{gd}^n - x_{id}^n\right)\right) \quad (6)$$

$$x_{id}^{n+1} = x_{id}^n + v_{id}^{n+1} \quad (7)$$

$$\omega^n = \frac{(\omega^{max} - \omega^{min}) * n}{n_{max}} \quad (8)$$

$$v^{min} \leq v_{id} \leq v^{max} \quad (9)$$

where $d = 1,\ldots,D$, with D the number of decision variables; i=1,…,N, with N the size of the swarm; r_1, r_2 are uniformly distributed random numbers in [0, 1]; n = 1, 2, . . ., the iteration number; c_1, c_2 acceleration coefficients that are, respectively, the cognitive and social components of the particle velocity, representing the impact of self-knowledge and the collective effect of the population; χ a constriction parameter which is employed, alternatively to the inertia parameter ω to limit the velocity to the range $[v^{min}, v^{max}]$.

By incorporating a recently proposed technique called Function Stretching into the classical PSO, Parsopoulos and Vrahatis [52] arrived at the SPSO method which has the capability to alleviate the attractions of local minima of the objective function and so to rise the success rates for finding a truly global solution of the problem.

The basic idea of SPSO is to use a two-stage transformation of the original objective function $f(x)$, which can be applied immediately after a local minimum $\bar{x}$ of the function $f(x)$ has been detected, defined as follows:

$$G(x) = f(x) + \gamma_1 \|x - \bar{x}\| \left(sign\left(f(x) - f(\bar{x})\right) + 1\right) \quad (10)$$

$$H(x) = G(x) + \gamma_2 \frac{sign\left(f(x) - f(\bar{x})\right) + 1}{tanh\left(\mu\left(G(x) - G(\bar{x})\right)\right)} \quad (11)$$

where γ_1, γ_2, and μ are arbitrary user-defined constants. The first transformation stage, $G(x)$ elevates the function $f(x)$, eliminating so most of the local minima, whereas the second stage, $H(x)$ stretches the neighborhood of $\bar{x}$ upwards, as it assigns higher function values to those points. The location of the global minimum is left unchanged, as both stages do not alter the local minima located below $\bar{x}$.

Further details of the implementation of the of CSPSO- methodology and its extension for solving the constrained optimization (CO) problem of the maximization of the net economic benefit of the total cultivated crops in the area under the constraints of limited water resources, water right priorities, and crop area limitations are present in the following sub-section.

3.7. Optimizing the agro-economic water productivity with CSPSO-MODSIM method

3.7.1. Formulation of the constrained optimization problem

The ultimate objective of the hydro-economic optimization model is to maximize the economic productivity of the sum of all crops in an irrigation plot under the constraints of limited water resources and crop areas available. By summing up Eq. 1 for all *cmax* crops, the objective function is:

$$Z = AEWP_t = \sum_{c'=1}^{cmax} AEWP_c = \sum_{c=1}^{cmax} \left[(Price_c * Y_c - Cost_c) * A_c \right] / Q_c^t, \quad (12)$$

(with the notations as given for Eq. 1) so that the optimization problem can be stated as follows:

$$Maximize\ Z \iff Minimize\ (-Z), \quad (13)$$

wherefore, for application of classical optimization (minimization) routines, like CSPSO, the objective function Z is replaced by its negative.

Peer-reviewed version available at Sustainability 2018, 10, 3953; doi:10.3390/su10113953

This, yet unconstrained optimization formulation will be extended to a constrained one by adding appropriate constraints as discussed below:

First of all, the actual crop yield Y_c entering Eq. 12 is dependent on the amount of irrigated water available which in turn depends on the actual water allocation (simulated by MODSIM). Thus, if the irrigation water amount delivered, Q_c, is less than the crop water requirement, ET_c, the actual crop yield, Y_c, will not reach its potential (maximum) crop yield $Ymax_c$. This is epitomized by the following FAO-equation [56]:

$$Y_c = Ymax_c * \left(1 - Ky_c * (1 - Q_c/ET_c)\right), \tag{14}$$

where $Ymax_c$ is the potential crop yield, estimated by SWAT as mentioned earlier, ET_c is the crop water requirement, Q_c is the MODSIM- simulated allocated irrigation water, Ky_c is a FAO-based yield response factor describing the effect of a reduction of irrigation water on the crops yield losses, with values gathered from Steduto et al. [57]. The crop water requirements ET_c were obtained using NetWat software from CropWat application series of the Iranian Water Directive (IWD) developed by the Iran government for estimating the effects of future climate change [58]. Eq. 14 shows clearly that unless the crop water requirement ET_C is fully met by irrigation water Q_c, the actual crop yield Y_c will be less than its potential crop yield $Ymax_c$.

The second kind of constraints for the optimization problem (14) model arises then firstly from the fact that the sum of all croplands cannot exceed the total arable area of the irrigation plot, i.e.

$$\sum_{i=1}^{7} A_{ZRBi} = At_{ZRB} \tag{15}$$

$$\sum_{i=1}^{7} A_{RKi} = At_{RK} \tag{16}$$

$$\sum_{i=1}^{2} A_{rchi} + \sum_{i=1}^{5} A_{gwi} = At_{ups} \tag{17}$$

where At_{ZRB} =684.2 km^2, At_{RK} = 125 km^2 and At_{ups} = 250km^2 are the future total arable areas supplied by the Boukan Dam irrigation network (ZRB) , of the RK plain and of the agricultural areas upstream of the dam, respectively, according to the SWAT- land use map and based on information of MOE [24]. The sums in Eqs. 15 to 17 run over 7 different areas, as this is the number of the major crops cultivated in the region which are, in alphabetic order, alfalfa, apple, barley, potatoes, sugar beets, tomatoes and wheat.

Further constraints which are varied later in the modelled scenarios pay attention to the fact that a high-benefit (low water costs) crops cannot be solely cultivated over the whole ZRB, but there are constraints on areas attributed to the various crops, not to the least to satisfy the population's food demands. More specifically, for each arable crop an allowable range of area size A_c is defined, wherefore the maximum values are taken from MOE [24] and for the minimum areal sizes two alternatives are investigated. In both of them, denoted as $Smin_1$ and $Smin_2$ in Table 1, the minimum areas devoted to the two cereals (barley, wheat) of the Boukan Dam network plot (BARL_ZRB and WWHT_ZRB) are set to the current arable area, whereas for the other crop/area demand nodes the minimum is assumed to have (1) no limitation (=0) for $Smin_1$, and (2) 60% of the maximum arable area for $Smin_2$. Based on these two numbers the corresponding areal sizes for the different crops have been computed for the different irrigation plots and listed in Table 1.

Table 1. Area constraints (km^2) for the two minimal-area scenarios ($Smin_1$ and $Smin_2$) devoted to the different crops for the three irrigation demand areas (ZRB, RK and upstream areas of the Boukan dam).

Crop/ area name	Amin		Amax	Crop /area name	Amin		Amax
	Smin1	Smin2			Smin1	Smin2	
ALFA_ZRB	0.0	19.9	154.2	SGBT_RK	0.0	3.0	5.1
APPL_ZRB*	109.2			TOMA_RK	0.0	5.1	8.4
BARL_ZRB	64.5	64.5	166.0	WWHT_RK	0.0	36.5	60.8
POTA_ZRB	0.0	10.9	35.6	APPL_gwdown*	2.1		
SGBT_ZRB	0.0	21.6	35.6	ALFA_gwup	0.0	14.2	23.7
TOMA_ZRB	0.0	14.5	59.3	POTA_gwup	0.0	3.3	5.5
WWHT_ZRB	237.6	237.6	415.1	SGBT_gwup	0.0	3.3	5.5
APPL_RK*	0.0			TOMA_gwup	0.0	5.5	9.1
ALFA_RK	0.0	13.2	22.0	BARL_rch	0.0	15.3	25.6
BARL_RK	0.0	14.2	23.6	WWHT_rch	0.0	38.4	63.9
POTA_RK	0.0	3.0	5.1				

Finally, as the production of cereal crops, i.e. barley (BARL) and wheat (WWHT) has a strategic importance in the ZRB as well as for Iran overall, three cereal crop pattern scenarios are considered further in this study, namely, that the sum of the cropland areas devoted to barley (A_{BARL}) and wheat (A_{WWHT}) will be a portion X of the maximum - minimum range above the minimum areas, i.e.:

$$A_{BARL}+A_{WWHT} \geq A_{min} + X * (A_{max}-A_{min}) \quad (18)$$

where X is the limiting production factor of the cereal crop pattern scenario and is set to, respectively, X=0.35, 0.5 and 0.65 for the three scenarios investigated, and A_{min} and A_{max} are the sum of the area limits of the different demand plots for the two crops (barley and wheat) (Table 1).

3.7.2. Integration of MODSIM and CSPSO algorithm

To solve the optimization problem, Eq. 13, subject to the four constraints, Eqs. 15- 18, by means of the CSPSO method, a penalty function method is used (e.g. [53]). The latter allows to convert a constrained optimization problem to an unconstrained optimization problem, by adding the constraints as a weighted penalty to the objective function (Eq. 13) in the form:

$$Minimize\ (-Z + h * \sum_{i=1}^{nc} PF_i) \quad (19)$$

where nc is the number of constraints, PF_i is the penalty factor of i-th constraint (Eqs. 15 - 19) which takes the binary values 0 or 1, depending on whether the constraint is satisfied or violated, respectively and h is the static penalty weighting factor value, which is found to be 10000 by trial and error based on a convergence analysis as well as PSO-literature recommended values.

Other parameters to be specified in the various CSPSO- equations of the previous sub-section are taken in agreement with recommended literature values as (e.g. [53,54]): N=40 (swarm size), n=500 (maximum iteration number); c_1=1.2 and c_2=0.8 (acceleration coefficients), γ_1=5000, γ_2 =0.5, μ = 10e^{-10} (three constraints of function stretching) and χ =1 (constriction parameter).

Finally, to arrive at the CSPSO-MODSIM integrated hydro- economic model (see Figure 3), the MODSIM water management tool is embedded in the CSPSO-optimization method as an inner layer of the iteration process. Thus, in the first iteration, the search algorithm generates the decision variables of the arable crop areas which should meet the ranges specified in Table 1. In the next step the water demands and their priorities are designated to the MODSIM- model based on the initial irrigation depth (estimated with SWAT) and the AEWPs (Eq. 1). Then, the optimal irrigation depths of the crops are estimated in MODSIM using Eqs. 2 to 4, with flow inputs from SWAT. The actual crop yields are predicted using Eq. 14 and returned to the CSPSO model, together with the optimal irrigation depths, to calculate the fitness/penalty function, Eq. 19. This procedure, coded in the MATLAB© environment, is repeated for each iteration of the CSPSO, using the swarm-intelligence, until the penalized objective function converges to the maximum net economic benefit of the total crop production in the three irrigation plots. Usually, after 400-500 iterations no noticeable further improvement in the objective function was obtained.

4. Results and discussion

4.1. Historical and future climate projections

The min. and max. temperatures- as well as the precipitation- predictors of the CGCM3 and CESM-CAM5 GCMs from the CMIP5-GCMs archive were found, respectively, by virtue of the skill score multi-criteria method, to be the most suitable climate predictors for further QM- downscaling [12].

The QM- downscaling model was calibrated and validated for each month of the year (e.g. January) for the time periods 1987-1998 and 1999-2005, respectively. The validation of the model was considered satisfactory, as the CDFs of the bias-corrected min/max temperatures and precipitation fit the CDF of the corresponding observed variables. In addition, the reliability of the QM- downscaled predictors was also evaluated by comparing them with the observed data for the period 2006-2015,

Peer-reviewed version available at *Sustainability* **2018**, *10*, 3953; doi:10.3390/su10113953

Table 2. Goodness of fitness measures of the QM-model for different RCPs for the time period 2006-2015.

Climate variable	Statistical measure	RCP scenario		
		RCP45	RCP60	RCP85
Temperature	R^2	0.81	0.88	0.78
	SE	5.80	3.75	6.10
	IA	0.91	0.95	0.88
Precipitation	R^2	0.23	0.31	0.19
	SE	24.2	21.1	23.5
	IA	0.68	0.81	0.63

using the goodness of fit measures coefficient of determination (R^2), standard error (SE) and index of agreement (IA) which are summarized for the three RCPs investigated in Table 2 (for further details see [12]).

Figure 5 shows the spatial distributions of the observed / QM- downscaled average annual temperatures and precipitation in the ZRB for the historical reference period (1987-2015).

GCM/QM-downscaled climate predictions for three RCP scenarios (RCP45, RCP60 and RCP85) are shown for three future periods, near (2020–2038), middle (2050–2068) and far future (2080– 2098), in Figures 6 - 8, respectively. One may notice from these figures that the trends in all future RCP-scenarios are approximately the same, such that, compared with the historical references period (see Figure 5), both the temperature and the precipitation are mostly increased.

In particular, for the near future period (Figure 6), the RCP45- and RCP60- scenarios turn out to be wetter than RCP85, wherefore RCP45 has a high precipitation increase coinciding with a moderate temperature rise, RCP60 practically no temperature rise, and RCP85 has a rather high temperature increase.

For the middle future period (Figure 7), and compared with the near future period (Figure 6), the RCP45-scenario will be drier again, going hand in hand with a small temperature rise, whereas RCP60 will become wetter while temperature will rise moderately. For RCP85, the trend is straightforward, with both a temperature and precipitation increase.

Finally, the far-future period (Figure 8) must be highlighted as most critical, as, compared with the middle-future period (Figure 7), on one hand, the temperature increases another 3% to 14% and, on the other hand, the precipitation decreases by another 4% to 22%, depending on the RCPs, with RCP85, as the most extreme, at the upper ends of these ranges.

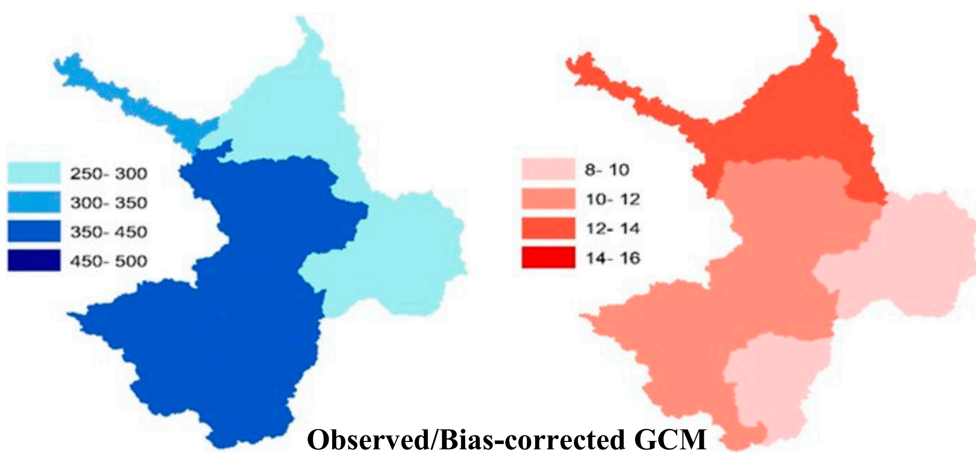

Figure 5. Spatial distributions of average 1987-2005 observed/bias corrected precipitation (left) and temperatures (right) in the ZRB.

doi:10.20944/preprints201808.0361.v1
Peer-reviewed version available at *Sustainability* **2018**, *10*, 3953; doi:10.3390/su10113953

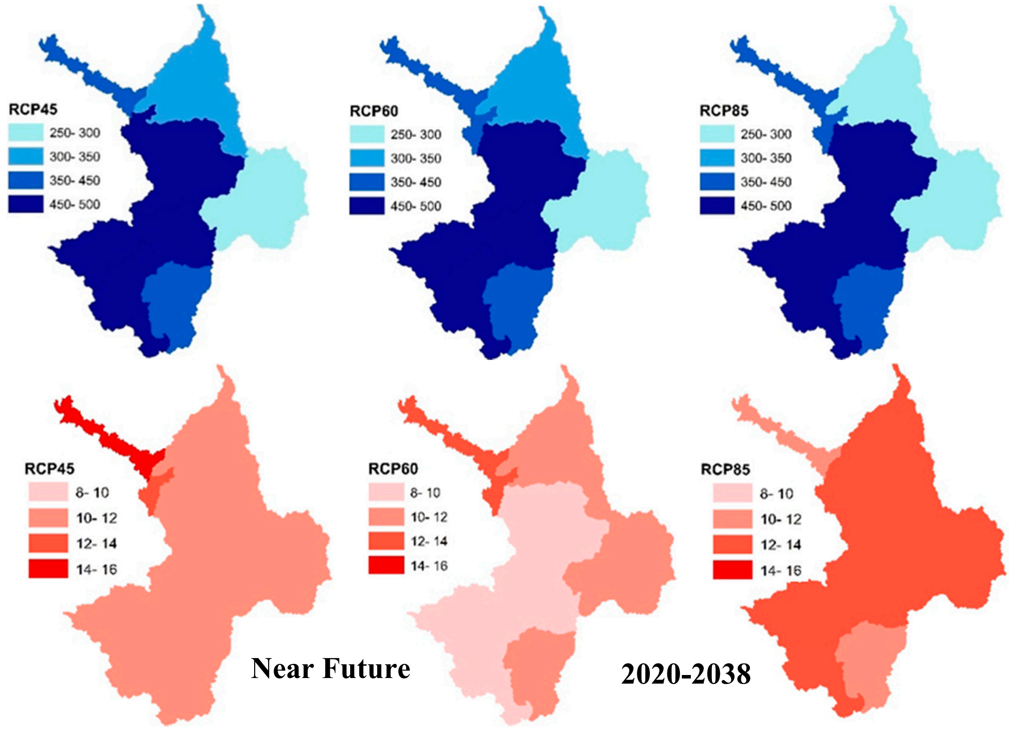

Figure 6. Spatial distributions of average precipitation (top) and temperature (bottom) in the ZRB during the near future period (2020-2038) for three RCPs.

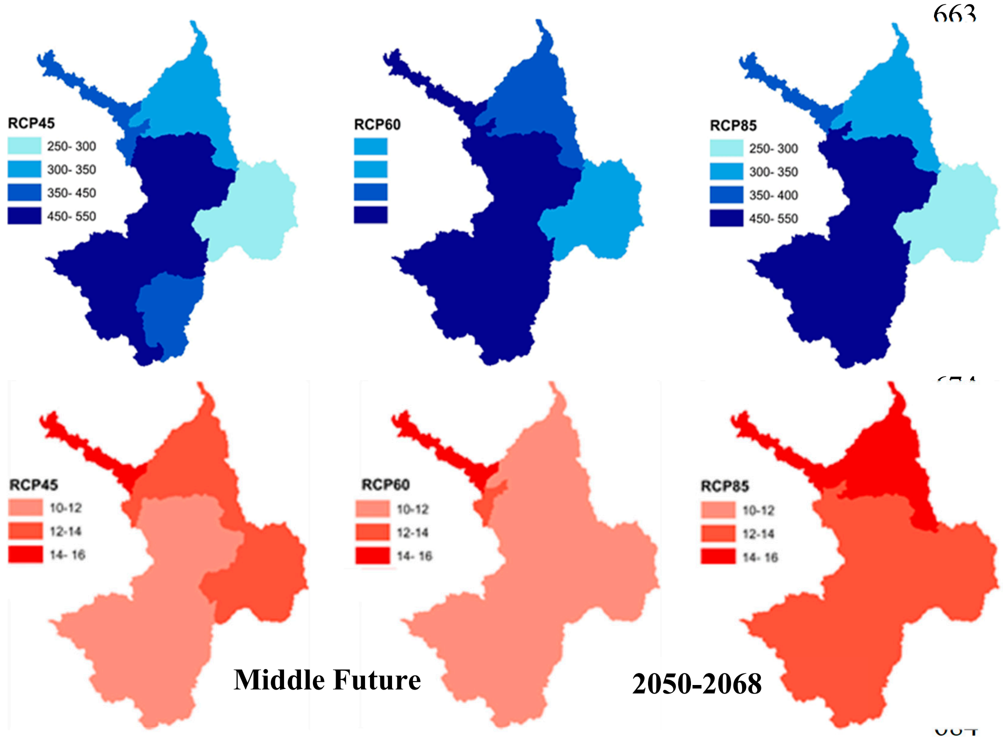

Figure 7. Similar to Figure 6, but for the middle future period (2050-2068).

Preprints (www.preprints.org) | NOT PEER-REVIEWED | Posted: 20 August 2018 doi:10.20944/preprints201808.0361.v1

Peer-reviewed version available at Sustainability 2018, 10, 3953; doi:10.3390/su10113953

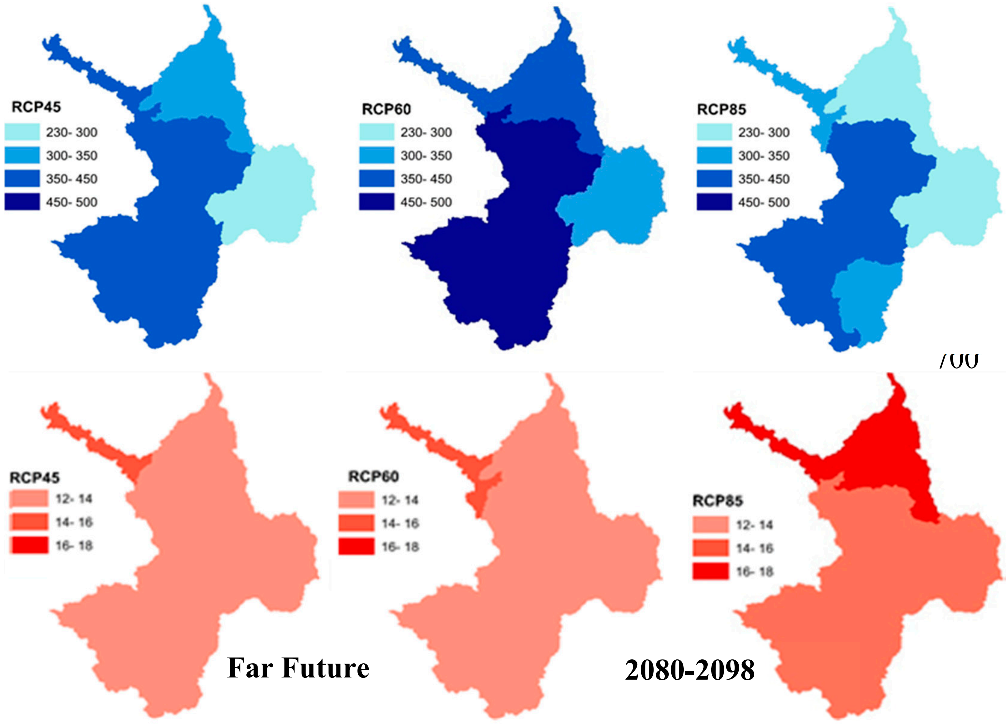

Figure 7. Similar to Figure 6, but for the far future period (2080-2098).

4.2. Climate change impacts on the hydrology of the ZRB

To evaluate the future climate impacts on the hydrology of the ZRB, the results of the statistics of the average annually accumulated of the SWAT-simulated monthly inflow to the Boukan Dam, starting from the minimum over various percentiles to the maximum, together with the resulting water balance components, surface runoff (*SWQ*), lateral subsurface flow (*LWQ*), groundwater inflow (*GWQ*) and water yield (*WYLD*), as taken from Emami and Koch [12], are presented for the three future periods under the three RCPs in Table 3.

As can be seen from the table, the highest increase and decrease of the annual dam inflow are predicted for RCP60 an RCP85, respectively. Compared with the minimum and the mean historical dam inflow, those values will be increased in the near and middle future, except for RCP45 in the near future, whereas they will decrease by 2% to 23% for the far future period. The maximum dam inflow will augment by 22% to 66% in the time period 2020- 2068, but decrease again by 6% to 31% after 2080. The low (25%) - quantile of the dam inflow will also experience a decrease, except for RCP45 in the middle future, whereas the high (75%) quantile will mostly increase, except of the far future period. The trends of the water balance components, e.g. of the water yield, are the same as the mean dam inflow.

The last column of Table 3 lists the Water Supply Stress Index *WaSSI* which is defined as the ratio of the total water demand *WD (*extracted from Emami and Koch[12]) (second to last column) of all sectors to the total water supply from surface and groundwater sources, i.e. the water yield *YWLD* (third to last column). Obviously, low values of *WaSSI* < 1 mean low water stress and *WaSSI*- values reaching 1 and above indicate high stress. Based on the *WaSSI*- indices computed in this way, Table 3 shows that the water stress in the ZRB will be higher than that of the historical period for the near- and middle-future periods and rise to an even alarming level (*WaSSI* >1) in the far-future period.

 doi:10.20944/preprints201808.0361.v1

Peer-reviewed version available at *Sustainability* **2018**, *10*, 3953; doi:10.3390/su10113953

Table 3. Statistics of the inflow of the Boukan dam, basin water balance components, total water demand (WD) (MCM/yr) and WaSSI- index for historic and future periods under different RCPs, with % -values denoting relatives to the historic reference period.

Scenario		Statistics with quantiles of dam inflow					Basin parameter					
		Min	25th Perc*	Mean	75th Perc*	Max	SURQ	GWQ	LATQ	WYLD	WD	WaSSI
Historic		154	704	990	1217	2213	46	84	38	2020	1375	0.68
Near	**RCP45**	-29%	-49%	-9%	-18%	66%	-13%	-18%	-16%	-16%	1288	0.76
	RCP60	>100%	-16%	29%	39%	49%	13%	5%	-8%	4%	1288	0.61
	RCP85	64%	-9%	21%	62%	27%	-24%	-2%	21%	-2%	1288	0.65
Middle	**RCP45**	27%	23%	44%	67%	22%	11%	15%	21%	15%	1373	0.59
	RCP60	2%	-41%	23%	47%	54%	2%	-2%	3%	1%	1373	0.67
	RCP85	58%	-8%	35%	62%	31%	2%	4%	24%	7%	1373	0.64
Far	**RCP45**	19%	-36%	-23%	-14%	-30%	-37%	-46%	-11%	-36%	1501	1.16
	RCP60	54%	-29%	-2%	12%	-6%	-24%	-32%	13%	-20%	1501	0.93
	RCP85	19%	-36%	-25%	-14%	-30%	-63%	-67%	-26%	-57%	1501	1.73

4.3. Crop yield simulation

As a major ingredient of the CSPSO-MODSIM crop pattern optimization model, the potential and actual crop yields of the major crops in the ZRB must be correctly known as these simulated and adjusted in the iterative optimization process, based on the prioritized water allocation and using FAO equation 14.

To simulate the crop production processes with the SWAT model, firstly the scheduled irrigation management operations are entered in its management module (.mgt). The most important management operations include planting, irrigation operation and harvest operation, for which the needed data has been taken from Ahmadzadeh et al. and MOE [23,24], i.e. the irrigation operations are defined for the HRUs with the major crops and using their monthly crop water requirements (ET_c), in terms of their irrigation depths, listed for the 7 crops in Table 4. These crop water depths are then later employed in the FAO equation, together with the available, prioritized water allocation Q_c, to update the actual crop yield in the CSPSO-MODSIM model iteration process.

The crop yields are computed in the SWAT-model based on crop parameters specified in the crop.dat input file. A set of initial crop yield effective parameters, described in Table 5, are adjusted based on literature values [23,59] and fine-tuned during the calibration/sensitivity analysis of the model to minimize the residuals of observed-simulated annual crop yields. The resulting final values of the crop parameters are also listed in Table 5. The SWAT- simulated crop yields are later applied as potential crop yields, $Ymax_c$ in the FAO equation (14), as it was found that the amount of irrigation water dispersed to a crop was more than compensating its crop water need so that the crop yields remained the same when an unlimited source of irrigation water was applied.

Using the calibrated crop parameters, the crop water requirements and the irrigation time scheme, as specified in Tables 4 and 5, the average crop yields over the time period 1987-2012 are simulated and compared with the observed average crop yields in the ZRB. The regression- and the bar- plot of Figure 9 indicate that the SWAT-model simulates the observed actuals crop yields - which as mentioned are in fact potential crop yields, $Ymax_c$ - in a satisfactory manner.

Preprints (www.preprints.org) | NOT PEER-REVIEWED | Posted: 20 August 2018 doi:10.20944/preprints201808.0361.v1

Peer-reviewed version available at Sustainability 2018, 10, 3953; doi:10.3390/su10113953

Table 4. Monthly crop water requirements (mm) for the major crops in the ZRB and their irrigation intervals (days).

Month	Crop						
	ALFA	APPL	BARL	POTA	SGBT	TOMA	WWHT
Apr	-	-	-	-	200	-	-
May	270	310	260	115	300	-	360
Jun	270	310	260	350	300	210	360
Jul	270	310	-	350	300	210	-
Aug	270	310	-	350	300	210	-
Sep	270	310	-	350	300	210	-
Sum	1350	1550	520	1515	1700	920	720
Irrigation interval (days)	15	15	10	10	10	10	10

Table 5. List of effective crop yield parameters adjusted in the SWAT-calibration process.

Parameter	Dimension	Definition	Final calibrated value						
			ALFA	APPL	BARL	POTA	SGBT	TOMA	WWHT
BLAI	m^2/m^2	Maximum potential leaf area index	5.0	5.5	3.4	4.5	5.0	4.5	4.0
HVSTI	Dimensionless	Harvest index for optimal growing conditions	0.7	0.6	0.3	1.15	2.0	1.4	0.4
DLAI	Dimensionless	Fraction of growing season when leaf area begins to decline	0.99	0.99	0.60	0.90	0.92	0.95	0.5
FRGRW1	Dimensionless	Fraction of the plant growing season corresponding to the 1st point on the optimal leaf area development curve	0.02	0.1	0.15	0.15	0.05	0.15	0.05
LAIMX1	m^2/m^2	Fraction of the maximum leaf area index corresponding to FRGRW1	0.01	0.4	0.01	0.10	0.05	0.50	0.05
FRGRW2	Dimensionless	Fraction of the plant growing season corresponding to the 1st point on the optimal leaf area development curve	0.15	0.5	0.45	0.30	0.5	0.35	0.45
LAIMX2	m^2/m^2	Fraction of the maximum leaf area index corresponding to FRGRW2	0.95	0.95	0.95	0.95	0.95	0.95	0.95
Tbase	°c	Minimum (base) temperature for plant growth	20	20	25	22	18	22	20
Topt	°c	Optimal temperature for plant growth	4	7	0	7	4	10	0
EXT_COEF	Dimensionless	Light extinction coefficient	0.57	0.65	0.65	0.65	0.65	1.0	0.65
BIO_E	$Kg.m^2$ (ha.MJ)	Radiation-use efficiency or biomass-energy ratio	16	50	35	45	30	60	30

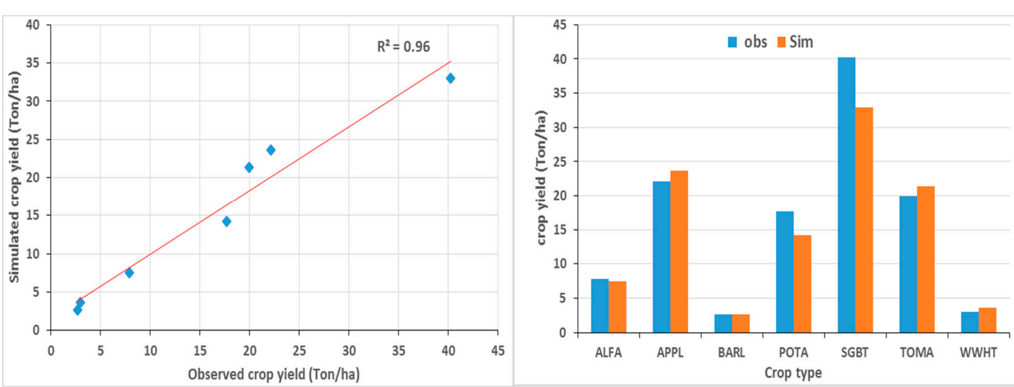

Figure 8. *SWAT- simulated and observed annual crop yields for 1987-2012. Left panel: Linear regression; right panel: bar chart.*

Preprints (www.preprints.org) | NOT PEER-REVIEWED | Posted: 20 August 2018 doi:10.20944/preprints201808.0361.v1

Peer-reviewed version available at *Sustainability* **2018**, *10*, 3953; doi:10.3390/su10113953

Table 6. Current selling prices, production costs, crop yields, crop areas, crop water requirements and initial AEWP of the major crops in the ZRB

Crop	ALFA	APPL	BARL	POTA	SGBT	TOMA	WWHT
Price (USD/kg)	0.21	0.07	0.25	0.13	0.06	0.14	0.32
Cost (USD/ha)	978	5501	420	1144	643	2056	503
Potential crop	7499	23627	2660	14235	22970	21391	3619
Area (km^2)	217	111	65	11	22	14	237
ET_c (mm)	1350	1550	520	1515	1700	920	720
AEWP (USD/m^3)	0.04	-0.14	0.05	0.05	0.04	0.09	0.09

4.4. Hydro-economic model analysis of optimal crop pattern

4.4.1. CSPSO- MODSIM model inputs

According to the CSPS-MODSIM model scheme of Figure 3, the crop- and water hydrological initial inputs of the hydro-economic model are as follows: potential crop yields (Figure 9), crop water requirements, i.e. the irrigation depths (Table 3), the SWAT-modeled inflow of the dam (SWAT-file output.std) and groundwater recharges (file output.rch).

For the economic analysis of the crop productions, the various crop economic values including the guaranteed selling price by the government, production costs, crop yields, crop areas, irrigation depths and AEWP of the major crops in the ZRB, gathered from [25,26] and listed in Table 6, are required.

The decision variables of the model are the cultivated areas (A_c) of the 7-1 major crops (the apple demand node is excluded, because an orchard cannot be replaced by other crops) in each of the three demand areas, i.e. there are 3*6= 18 variables, as shown in Figure 4.

In the next step, the CSPSO-MODSIM algorithm generates initial values for these 18 decision variables, depending on the ranges of the individual crop areas for the two minimum area scenario (Smin$_1$ and Smin$_2$) as specified in Table 1. Then the MODSIM- model will be run starting with the initial sum of agricultural water productivities, $AEWP_c$ (Eq. 12), based on the current conditions (see Table 6). In the next step, the allocated water for each crop will be captured from the MODSIM model and, using the FAO Eq. 14, the actual crop yield and the main objective function Z, i.e. the total $AEWP_t$ (Eq. 12), will be estimated (updated) and the process repeated as part of the iteration scheme of the CSPSO- MODSIM process, wherefore the decision variables (crop areas) are adjusted based on the CSPSO- swarm information, until the maximum (=negative minimum) net economic benefit per unit water supply (= total $AEWP_c$) will be reached.

From Table 6 one may notice that the sum of the $AEWP_c$ for the current crop areas situation is very low, with only about 0.347 USD/m^3 , excluding APPL, which is an orchard and it is not considered in the multi-crop optimization model and just applied as a demand node in the MODSIM model. In fact, APPL has a negative $AEWP_c$ which means that its production cost is more than its selling price. In contrast, TOMA and WWHT have the highest- and BARL and POTA the lowest-, but still positive agricultural economic water productivities $AEWP_c$.

4.4.2. Optimization of crop pattern areas for the different cultivation area- and cereal production constraints for different future periods and RCPs

4.4.2.1. Optimal AEWP$_t$- objective functions for different scenarios

The CSPSO-MODSIM simulation- optimization model is run under the two minimum arable cultivation-area constraints (Smin$_1$ and Smin$_2$, see Table 1) and three different possible levels of cereal production rates (X=50%, 35% and 65%) to find the most suitable crop pattern, i.e. the one providing the maximum net economic benefit per unit water supply, $AEWP_t$. This process is repeated for the

Peer-reviewed version available at *Sustainability* **2018**, *10*, 3953; doi:10.3390/su10113953

Table 7. Optimal Z (=total $AEWP_t$)- values (USD/m^3) for three kinds of cereal production-rates (X=35%, 50% and 65%) under the two minimum arable cultivations areas constraints ($Smin_1$ and $Smin_2$) for three future periods and three RCPs.

$Smin_1$						$Smin_2$					
RCP	**Future period**	**X 35%**	**X 50%**	**X 65%**	**Selected**	**RCP**	**Future period**	**X 35%**	**X 50%**	**X 65%**	**Selected**
RCP 45	Near	0.88	1.05	1.07	X= 65%	RCP 45	Near	1.29	1.31	0.98	X= 50%
	Middle	1.00	0.91	1.00			Middle	1.31	1.32	1.32	
	Far	0.85	0.89	0.84			Far	0.93	0.94	1.00	
Average		0.91	0.95	0.97		Average		1.18	1.19	1.10	
RCP 60	Near	0.98	1.05	0.93		RCP 60	Near	1.41	1.07	1.06	X= 35%
	Middle	1.03	0.98	0.87			Middle	1.14	1.14	1.19	
	Far	1.04	1.09	0.90			Far	1.02	1.02	1.01	
Average		1.02	1.04	0.90		Average		1.19	1.08	1.09	
RCP 85	Near	0.97	0.94	0.87		RCP 85	Near	0.97	0.94	0.91	X= 50%
	Middle	0.97	0.99	0.87			Middle	1.05	1.01	1.02	
	Far	0.97	0.92	1.21			Far	0.98	1.18	1.11	
Average		0.97	0.95	0.98		Average		1.00	1.04	1.01	

three RCPs and three future periods. The results are shown in Table 7, wherefore for simplification and strategic implications the results in each group have been averaged over all three future time periods.

As can be seen from Table 7, for the $Smin_1$ –minimum crop area scenario, the 65%- rate for cereal production is recommended over the total future period (up to year 2100) and this holds all three RCPs. However, as in this $Smin_1$- scenario the minimum cultivated area for all non-cereal crops is set to zero (see Table 1), such a drastic extension of the cereal cultivation area may not generally be acceptable and will more likely increase the social dissatisfaction of the farmers and stakeholders in that region. In contrasts, for the $Smin_2$ –scenario the optimal cereal production turns out to be only 50% for both RCP45 and RCP85, but only 35% for RCP60, i.e. the cereal production areas will not be extended that much. Therefore, and also because of the higher optimal $AEWP_t$ for the $Smin_2$ – than for the $Smin_1$- scenario, the results of $Smin_2$ are favored here and will be discussed in more detail in the following. Thus one may notice from the table that the average optimal $AEWP_t$ s for the medium-emission scenarios, RCP45 and RCP60, are with ~1.2 USD/m^3 about the same, whereas for the high-emission scenario, RCP85, it is about 9 % lower.

4.4.2.1.1. Optimal simulated future optimal crop pattern for crop-area constraint $Smin_2$

For a proper appraisal of the simulated future optimal crop pattern proportions, the historical ones, retrieved from a current land-use map of the study region, are presented in the two pie-charts of Figure 10 for the Boukan Dam network demand area (_ZRB) as well as the upstream demand area of the dam (_gwup and _rch) (see Figure 4, for notations). As the RK-Plain is assumed as a developing agricultural demand only for the future, it is not considered here. These pie-charts indicate that the major crops in the ZRB as a whole are WWHT, ALFA, BARL, SGBT, TOMA and POTA, in descending order. The future optimal crop pattern proportions of the ZRB basin are presented in three pie charts of the Figure 11 to Figure 13 for RCP45, RCP60 and RCP85, which are based on the average of three future periods and the selected cereal production limit (*X*) from Table 7.

Preprints (www.preprints.org) | NOT PEER-REVIEWED | Posted: 20 August 2018 doi:10.20944/preprints201808.0361.v1
Peer-reviewed version available at Sustainability 2018, 10, 3953; doi:10.3390/su10113953

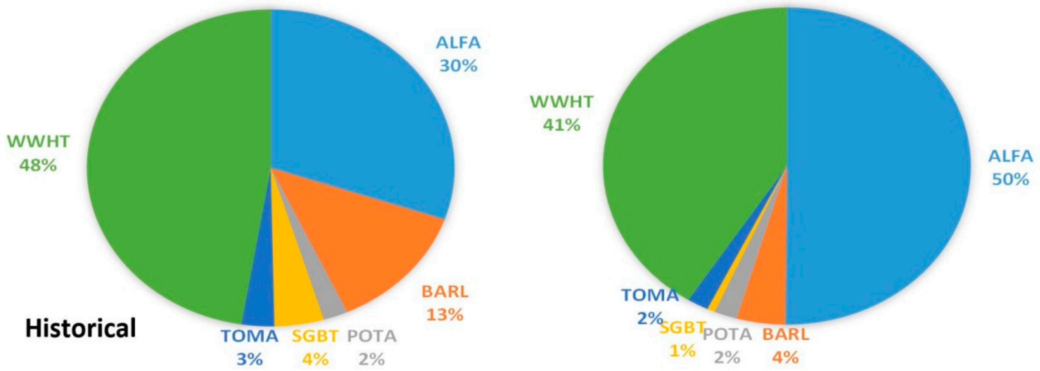

Figure 9. *Current/historic crop pattern proportions of the Boukan Dam network- (left pie) and the upstream of the dam demand area (right pie).*

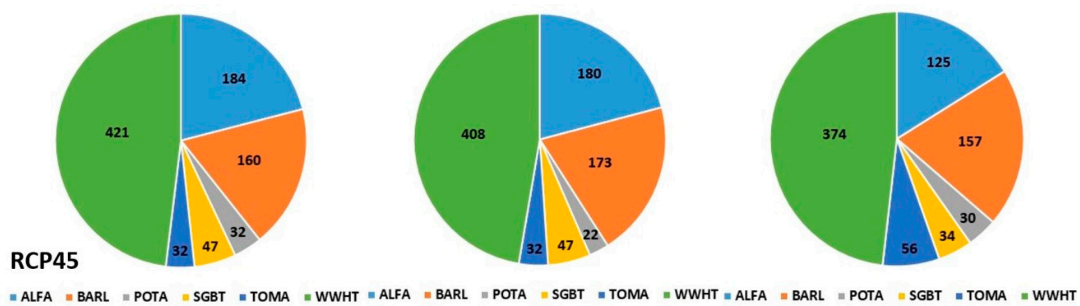

Figure 10. *Optimal crop pattern for RCP45 for the three future periods: the near (left panel), middle (middle panel) and far (right panel) future.*

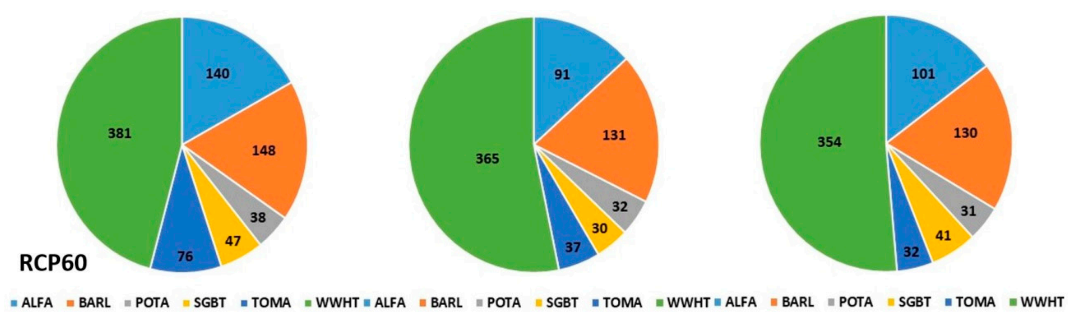

Figure 11. *Similar to Figure 11, but for RCP60.*

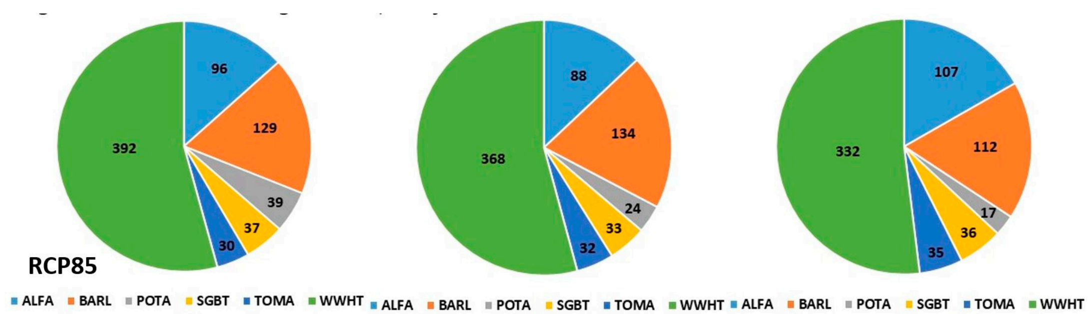

Figure 12. *Similar to Figure 11, but for RCP85.*

Preprints (www.preprints.org) | NOT PEER-REVIEWED | Posted: 20 August 2018 doi:10.20944/preprints201808.0361.v1

Peer-reviewed version available at Sustainability 2018, 10, 3953; doi:10.3390/su10113953

Table 8. Optimal crop areas (km²) for the Smin$_2$- scenario and the optimal cereal area constraints selected (X- %) for the three RCPs for the three future periods (near, middle, far) based on the optimal AEWP$_t$ – values found in Table 6.

Irrigation plot	Crop	RCP45 / X-50%			RCP60/ X-35%			RCP85/ X-50%		
		near	middle	far	near	middle	far	near	middle	far
Boukan dam network	ALFA	139	135	90	95	59	71	69	58	72
	BARL	110	123	119	98	102	101	92	100	74
	POTA	21	11	24	28	21	25	31	14	8
	SGBT	36	36	28	36	22	35	31	24	27
	TOMA	15	15	44	59	22	15	16	16	22
	WWHT	322	309	282	282	271	259	317	290	256
RK plain	ALFA	21	21	15	21	13	13	13	14	17
	BARL	24	24	14	24	14	14	18	16	18
	POTA	5	5	3	5	5	3	3	5	4
	SGBT	5	5	3	5	3	3	3	4	4
	TOMA	8	8	6	8	8	8	5	7	6
	WWHT	61	61	54	61	56	57	37	40	47
Boukan dam upstream area	ALFA	24	24	20	24	19	17	14	16	18
	BARL	26	26	24	26	15	15	19	18	20
	POTA	6	6	3	5	6	3	5	5	5
	SGBT	6	6	3	6	5	3	3	5	5
	TOMA	9	9	6	9	7	9	9	9	7
	WWHT	38	38	38	38	38	38	38	38	29
Total arable area		876	862	776	830	686	689	723	679	641

In addition, the optimum values of the 18 decision variables of the CSPSO-MODSIM model i.e. the recommended arable areas of the major crops in the three irrigation plots (A_c), are listed in Table 8 for different RCPs and 2020-2038, 2050-2068 and 2080-2098 future periods.

As can be seen in the Table 8, although the arable area is on average increased from 632 km² to 838, 735 and 680 km² for RCP45, RCP60 and RCP85 respectively, it is recommended that the ALFA crop area should be decreased from 15% to 59% because of low agro-economic water productivity and high consumption of this crop. For fulfilling the demands of the alfalfa production in the region Naraqi et al. [43] recommended to cultivate the alfalfa in the riverside of Aras River which is more suitable for this crop and then transfer it to which is expected to be more efficient in economic and water resources point of view.

One may notice that the two cereals, WWHT and BARL have the most increase of arable area, 72 and 86 km² respectively on average, according to their importance as a strategic crop of the ZRB which is applied as cereal crop pattern scenario to the constraints.

In comparison with the historical crop cultivated areas, the SGBT has the lowest development regarding their rather high consumption of water and low AEWP, whereas the TOMA and POTA shares of crop pattern have respectively the most proportional increase for the average of different RCPs because of the rather high AEWP and lower water demand.

As expected the lowest agricultural development is recommended for far future- RCP85 scenario, whereas the highest area extension is for RCP45 in the near future period. For RCP60 and RCP85 the highest relative increase in percent is in the POTA and TOMA crop proportions, but for for RCP45 in BARL and TOMA crops.

Preprints (www.preprints.org) | NOT PEER-REVIEWED | Posted: 20 August 2018 doi:10.20944/preprints201808.0361.v1

Peer-reviewed version available at *Sustainability* **2018**, *10*, 3953; doi:10.3390/su10113953

Table 9. *Total annual economic benefits (in 1000 USD) for the optimal crop pattern distribution for the three future time periods under the three RCPs.*

Future period	2020-2038 (near)			2050-2068 (middle)			2080-2098 (far)		
RCP scenario	RCP45	RCP60	RCP85	RCP45	RCP60	RCP85	RCP45	RCP60	RCP85
Annual economic benefits	598.5	682.6	414.9	751.2	642.0	431.2	418.5	442.5	414.3

The corresponding annual economic benefits of the recommended crop patterns are also presented in Table 9 in 1000 USD for different RCPs and future scenarios. As expected, RCP45 and RCP60 are estimated to have the rather higher economic benefits up to 2068 unlike of RCP85. For all RCPs the net economic benefits are averagely increased from near to middle future period, whereas the least average economic values are expected to be in the far future period, 2080-2098.

4.4.2.1.2. Optimal future crop water irrigation depths

The average annual crop water irrigation depths IRR_c delivered, in % relative to the crop water demands ET_c, of the historic reference period (see Table 4) for the optimal crop pattern under area limitation constraints *$Smin_2$* are listed in Table 10 for the three future periods under the three RCPs. The table indicates that for the note of the future periods and RPCs is the irrigation water supplied able to satisfy the crops water demand for the historic period. In fact, the overall crop water demands are supplied on average by only 60% - 79% for RCP45, 61% - 79% for RCP60 and 49% - 76%, i.e. the future water resources in the basin are too limited to support the agriculture up to its full potential. The table shows also that relative to the crop water demands of the reference period, for the future periods these are satisfied less for barley and sugar beet than for the other crops, wherefore tomato and potato crop water demands are supplied at the highest rates.

Based on the annual percentages of Table 10, the future the optimal irrigation depths (IRR_c) are estimated on the monthly scale by multiplying the monthly crop water requirements, Et_c of Table 4 by the corresponding percentage factors. As an example, the results are listed for the scenario RCP45 and the middle future period in Table 11.

Table 10. Average annual crop water irrigation depths IRR_c supplied in % relative to the crop water demands ET_c, of the historic reference period (Table 4) (in mm/yr) for the optimal crop pattern under $Smin_2$ –constraint for the future periods under the three RCPs.

Period	**RCP**	**Crop**					
		ALFA	**BARL**	**POTA**	**SGBT**	**TOMA**	**WWHT**
	Historic	1350	520	1515	1700	920	720
Near	RCP45	57%	44%	59%	49%	83%	66%
	RCP60	53%	42%	68%	49%	84%	67%
	RCP85	78%	56%	69%	78%	82%	70%
Middle	RCP45	66%	52%	60%	53%	57%	75%
	RCP60	78%	60%	80%	74%	76%	71%
	RCP85	82%	57%	79%	82%	86%	71%
Far	RCP45	84%	66%	78%	82%	85%	79%
	RCP60	81%	67%	88%	77%	82%	76%
	RCP85	55%	41%	50%	48%	52%	48%

Preprints (www.preprints.org) | NOT PEER-REVIEWED | Posted: 20 August 2018 doi:10.20944/preprints201808.0361.v1

Peer-reviewed version available at Sustainability 2018, 10, 3953; doi:10.3390/su10113953

Table 11. Optimal monthly irrigation water (mm) applied for the different crops for RCP45 in the middle future (2050- 2068) period.

Month	Crop					
	ALFA	**BARL**	**POTA**	**SGBT**	**TOMA**	**WWHT**
Apr	-	-	-	106	-	-
May	178	135	69	159	-	270
Jun	178	135	210	159	120	270
Jul	178	-	210	159	120	-
Aug	178	-	210	159	120	-
Sep	178	-	210	159	120	-
Sum	891	270	909	901	480	540
Irrigation interval	15	10	10	10	10	10

4.4.2.1.3. Implications and concluding remarks

Interestingly, in connection with the above results, it has been recommended by the Urmia Lake Restoration Committee [60] to decrease the agricultural demands of the LU basin by 40%, based on new executive strategies of demand management to avoid an imminent ecological and environmental disaster of the lake and the surrounding ecosystem. In fact, such a reduction of the future agricultural water irrigation is approximately found here as, following Table 10, about 60% of the total agricultural demands of ZRB can be supplied for the RCP45 and RCP85 scenarios.

The LU- disaster mitigation strategies include an increase of the irrigation efficiency, better river bed and bank management, deficit irrigation, improvement of the Zarrine irrigation network and completion of irrigation secondary networks with surface and modern techniques and last, but not least, suggestions to replace some high water-consuming crops like SGBT with some less consuming ones such as Canola.

Regarding the crop water demands of the apple orchards, it should be noted that they are not met in some months, as the water planning model allocates water based on the $AEWP_c$ and which based on the potential crop yield was is calculated to be negative for apple and, therefore, will have the least priority in the agricultural demand chain. It has also been proposed by Naraqi et al. [43] to replace parts of the orchards with crops with more economic benefits and less water use such as Canola, Pistachio or Saffron. The initial $AEWP_c$ of these crops are listed in Table 12 [25,26] and they are indeed several times higher than the initial $AEWP_C$ of the ZRB major crops (see Table 6) analyzed heretofore.

Table Error! No text of specified style in document.**.12.** Selling prices, production costs, crop yields, crop areas, crop water requirements and initial $AEWP_c$ of additional crops recommended for cultivation in the ZRB.

Crop specification	**Canola**	**Pistachio**	**Saffron**
Price (USD/kg)	0.5	7	1750
Cost (USD/ha)	329	4020	7250
Potential crop yield (kg/ha)	1998	650	5
ET_c (mm)	659	500	300
AEWP (USD/m^3)	0.10	0.11	0.21

5. Summary and Conclusions

In this paper, an integrated hydro- economic model is developed as a crop pattern and irrigation planning tool using a combination of QM, SWAT and MODSIM simulation models with the Constrained Stretched Particle Swarm Optimization (CSPSO) optimization search algorithm. The objective of the study is to optimize the future crop pattern of the major crops in the ZRB and their crop water irrigation depths in terms of net economic benefits and crop water productivity, considering the impact scenarios of the climate change and the cereal crop pattern scenarios. To do this, the weather climate change scenarios are first predicted using a statistical downscaling method, two- step updated QM (Quantile Mapping) bias correction technique based on the most suitable GCM outputs for the min./max. temperatures and precipitation namely CGCM3 and CESM-CAM5 of CMIP5 archive to assess the impact scenarios of the climate change (RCP 45, 60 and 85) in three 19-years future periods (near, middle and far). In the next step the downscaled weather variables are applied to the calibrated and validated basin-wide hydrologic model, SWAT, to simulate the future available water resources including the reservoir inflow and hydrologic changes. The crop yield potentials are also simulated using the SWAT model with applying the irrigation depths based on their monthly crop water requirements and adjusting the crop parameters. To setup a water planning simulation module, the MODSIM model is then customized to allocate water based on AEWP index of the major crops i.e. the combination of crop water productivity and production economic benefit. Finally, the CSPSO-MODSIM simulation- optimization model is developed with coupling this customized MODSIM model with a Constrained SPSO optimization algorithm with the objective function of optimizing the total AEWP ($AEWP_t$) under constraints of the different cereal crop pattern scenario and the arable area ranges for the irrigation plots including Boukan Dam network, upstream of the dam and RK Plain. A penalty function method is employed to convert the constrained optimization problem to an unconstrained optimization solved using SPSO algorithm. As main output of the model, the optimal crop cultivable areas and corresponding irrigation schedule up to year 2098 are determined for each impact scenario of climate change (RCP 45, 60 and 85) which will maximize the net economic benefits and the crop water productivity of the ZRB crops simultaneously considering the possible impacts of climate change and cereal crop production scenarios.

According to the predicted impacts of climate change, RCP60 an RCP85 are expected to have the highest increase and decrease respectively in the inflow of the dam. For all RCPs the Boukan Dam inflow will be increased in the near and middle future in comparison with the minimum and the mean historical dam inflow, except for RCP45 in near future, whereas it is predicted that they will have a decrease by 2% to 23% for the far future period. The lowest available water resources are predicted for the far future regarding rather low precipitation and high temperature, especially RCP85 which has the highest decrease of freshwater. The performance of the SWAT model for the streamflow and the crop yield simulation is quite satisfactory. The ratio of water demand across the water supply i.e. the WaSSI indices of the ZRB- simulated scenarios are predicted to be higher than the historical period for the near and medium periods, while the highest water stress is expected for the far future period.

Based on the optimal results of the developed hydro-economic CSPSO-MODSIM model, the total agro- economic water productivity of the major crops of basin (except of APPL) are improved considerably from 0.36 USD/m^3 to 1.04 (RCP45) to 1.19 USD/m^3 (RCP45 and RCP60) which means the economic benefits of the crop production per unit supplied water is approximately tripled using this integrated algorithm. Regarding low AEWP and high water demand of ALFA crop, its cultivated area should be decreased gradually and maybe it is more efficient economically to export it from a neighbour catchment, such as Aras River Basin. One may notice that the WWHT and BARL share of crop pattern have the most increase of arable area, owing to the cereal crop pattern scenario which is applied as a constraint of the model and also their rather high simulated AEWP and low water demand. The TOMA and POTA shares of crop pattern have respectively the most proportional increase for the average of different RCPs in comparison with the historical period crop pattern due to their relatively higher water productivity (AEWP), whereas the SGBT has the lowest rise according to quite high consumption of water and low simulated AEWP.

In addition, the evaluation of model outputs for the climate change scenarios indicated that for the medium emission scenario (RCP45 and RCP60) the economic return will be quite high up to 2068 with applying this hydro-economic method, whereas for the high emission scenario (RCP85) is expected to have less net economic benefit. However, it is expected to have the least economic return in 2080-2098 years for all RCPs. The arable areas of the crops are extended more or less in the future years in to supply the food security of the ZRB, which the highest and lowest increase is for near-RCP45 and far-RCP85 scenarios. Comparing the optimal crop pattern with the historical crop pattern proportions, the highest relative increase will be in the POTA and TOMA crops for RCP60 and RCP85, and in BARL and TOMA crops for RCP45.

Furthermore, it is recommendable to replace the high consuming water and low agro-economic water productivity crops such as ALFA, APPL and SGBT with the crops with less water demand and higher economic benefits like other major crops of ZRB or some new cultivable region- specific crops of the ZRB such as Canola, Saffron and Pistachio.

Based on the proposed research, a basin-wide integrated hydro- economic model is provided for additional studies of the irrigated agricultural lands integrating the agricultural economic and water resources management concepts, in order to better respond to the future water variability due to the climate change and the unsustainable use of water. The developed approach could be used to analyse a high-resolution analysis of an agriculturally exploited basin located in an arid or semi-arid area.

This integrated model is able to support water resources authorities and other stakeholder in a water-scarce basin as a sustainable water decision making tool, to find the most suitable regional management strategies i.e. the optimal different water uses and optimal land use planning scenario for the future years. However, the accuracy of the model can be improved with using another crop yield forecasting method such as estimation of different Ky for the each stage of crop growth or considering all the spatial and temporal changes of the land use classes and their related water demands in the model.

Author Contributions: Manfred Koch supervised the research. Farzad Emami conceived the research, implemented the procedures and wrote the outline of the manuscript. Both authors contributed in finalizing the manuscript, with Manfred Koch doing the final major editing.

Conflicts of Interest: The authors declare no conflicts of interest.

References

1. OCHA, U. In *Water scarcity and humanitarian action: Key emerging trends and challenges, un*, UN. World Economic Forum,"Global Risks"(2014), World Economic Forum, 2010.
2. Mo, X.-G.; Hu, S.; Lin, Z.-H.; Liu, S.-X.; Xia, J. Impacts of climate change on agricultural water resources and adaptation on the north china plain. *Advances in Climate Change Research* **2017**, *8*, 93-98.
3. Voss, K.A.; Famiglietti, J.S.; Lo, M.; Linage, C.; Rodell, M.; Swenson, S.C. Groundwater depletion in the middle east from grace with implications for transboundary water management in the tigris-euphrates-western iran region. *Water resources research* **2013**, *49*, 904-914.
4. Dubois, O. *The state of the world's land and water resources for food and agriculture: Managing systems at risk*. Earthscan: 2011.
5. Mesgaran, M.B.; Madani, K.; Hashemi, H.; Azadi, P. Iran's land suitability for agriculture. *Scientific reports* **2017**, *7*, 7670.
6. van Arendonk, A. The development of the share of agriculture in gdp and employment. **2015**.
7. Motamed, M. Developments in iran's agriculture sector and prospects for us trade. **2017**.

8. Rafiei Emam, A., Impact of climate and land use change on water resources, crop production and land degradation in a semi-arid area (using remote sensing, GIS and hydrological modeling). Doctoral program of Geoscience/Geography,The Georg- August University School of Science (GAUSS), February 2015.
9. Conforti, P. *Looking ahead in world food and agriculture: Perspectives to 2050*. Food and Agriculture Organization of the United Nations (FAO): 2011.
10. Alexandratos, N.; Bruinsma, J. *World agriculture towards 2030/2050: The 2012 revision*; ESA Working paper FAO, Rome: 2012.
11. Abbaspour, K.C.; Faramarzi, M.; Ghasemi, S.S.; Yang, H. Assessing the impact of climate change on water resources in iran. *Water resources research* **2009**, *45*.
12. Emami, F.; Koch, M. Evaluation of statistical-downscaling/bias-correction methods to predict hydrologic responses to climate change in the zarrine river basin, iran. *Climate* **2018**, *6*, 30.
13. Chijioke, O.B.; Haile, M.; Waschkeit, C. Implication of climate change on crop yield and food accessibility in sub-saharan africa. *Centre for Development Research. Bonn: University of Bonn* **2011**.
14. Ashraf Vaghefi, S.; Mousavi, S.; Abbaspour, K.; Srinivasan, R.; Yang, H. Analyses of the impact of climate change on water resources components, drought and wheat yield in semiarid regions: Karkheh river basin in iran. *hydrological processes* **2014**, *28*, 2018-2032.
15. Teshager, A.D.; Gassman, P.W.; Schoof, J.T. Assessment of impacts of agricultural and climate change scenarios on watershed water quantity and quality, and crop production. *Hydrology and Earth System Sciences* **2016**, *20*, 3325.
16. Bou-Fakhreddine, B.; Abou-Chakra, S.; Mougharbel, I.; Faye, A.; Pollet, Y. In *Optimal multi-crop planning implemented under deficit irrigation*, Electrotechnical Conference (MELECON), 2016 18th Mediterranean, 2016; IEEE: pp 1-6.
17. Fazlali, A.; Shourian, M. A demand management based crop and irrigation planning using the simulation-optimization approach. *Water Resources Management* **2018**, *32*, 67-81.
18. Fredericks, J.W.; Labadie, J.W.; Altenhofen, J.M. Decision support system for conjunctive stream-aquifer management. *Journal of Water Resources Planning and Management* **1998**, *124*, 69-78.
19. Fereidoon, M.; Koch, M. Swat-modsim-pso optimization of multi-crop planning in the karkheh river basin, iran, under the impacts of climate change. *Science of The Total Environment* **2018**, *630*, 502-516.
20. Keshavarz, A.; Heydari, N.; Ashrafi, S. In *Management of agricultural water consumption, drought, and supply of water for future demands*, proceedings of the Seventh International Conference on the Development of Dryland, 2003; pp 42-48.
21. ULRP. Challenges of urmia lake and restoration program. International cooperation division. *International Cooperation Division. Tehran: Urmia Lake Restoration Program (ULRP)* 2017.
22. Ministry of Agriculture. Agricultural statistics and the information center. Tehran, Iran, 2007.
23. Ahmadzadeh, H.; Morid, S.; Delavar, M.; Srinivasan, R. Using the swat model to assess the impacts of changing irrigation from surface to pressurized systems on water productivity and water saving in the zarrineh rud catchment. *Agricultural Water Management* **2016**, *175*, 15-28.
24. Ministry of the Energy (MOE). Updating of water master plan of iran; water and wastewater macro planning bureau: Tehran, iran. 2014.
25. Ministry of Agriculture (MOA). Agriculture Statistics: Volume 1, Field Crops, Iranian Ministry of Agriculture (2014–2015).2015.
26. Statistical centre of Iran (SCI). Available online: www.amar.org.ir. (accessed on 30.06.2018).

27. Harou, J.J.; Pulido-Velazquez, M.; Rosenberg, D.E.; Medellín-Azuara, J.; Lund, J.R.; Howitt, R.E. Hydro-economic models: Concepts, design, applications, and future prospects. *Journal of Hydrology* **2009**, *375*, 627-643.
28. Taylor, K.E.; Stouffer, R.J.; Meehl, G.A. An overview of cmip5 and the experiment design. Bulletin of the American Meteorological Society 2012, 93, 485-498.
29. Pachauri, R.K.; Allen, M.R.; Barros, V.R.; Broome, J.; Cramer, W.; Christ, R.; Church, J.A.; Clarke, L.; Dahe, Q.; Dasgupta, P. *Climate change 2014: Synthesis report. Contribution of working groups i, ii and iii to the fifth assessment report of the intergovernmental panel on climate change*. IPCC: 2014.
30. Hempel, S.; Frieler, K.; Warszawski, L.; Schewe, J.; Piontek, F. A trend-preserving bias correction–the isi-mip approach. *Earth System Dynamics* **2013**, *4*, 219-236.
31. Miao, C.; Su, L.; Sun, Q.; Duan, Q. A nonstationary bias-correction technique to remove bias in gcm simulations. *Journal of Geophysical Research: Atmospheres* **2016**, *121*, 5718-5735.
32. Neitsch, S.L.; Arnold, J.G.; Kiniry, J.R.; Williams, J.R. *Soil and water assessment tool theoretical documentation version 2009*; Texas Water Resources Institute: 2011.
33. Jha, M.; Pan, Z.; Takle, E.S.; Gu, R. Impacts of climate change on streamflow in the upper mississippi river basin: A regional climate model perspective. *Journal of Geophysical Research: Atmospheres* **2004**, *109*.
34. Abbaspour, K.C.; Johnson, C.; Van Genuchten, M.T. Estimating uncertain flow and transport parameters using a sequential uncertainty fitting procedure. *Vadose Zone Journal* **2004**, *3*, 1340-1352.
35. Krause, P.; Boyle, D.; Bäse, F. Comparison of different efficiency criteria for hydrological model assessment. *Advances in geosciences* **2005**, *5*, 89-97.
36. Moriasi, D.N.; Arnold, J.G.; Van Liew, M.W.; Bingner, R.L.; Harmel, R.D.; Veith, T.L. Model evaluation guidelines for systematic quantification of accuracy in watershed simulations. *Transactions of the ASABE* **2007**, *50*, 885-900.
37. Abbaspour K.C.; Yang J.; Maximov I.; Siber R.; Bogner K.; Mieleitner J.; Zobrist J.; Srinivasan, R. Modelling hydrology and water quality in the pre-alpine/alpine Thur watershed using SWAT. *Journal of hydrology*. **2007**, 333, 413-30.
38. Srinivasan, R.; Zhang, X.; Arnold, J. Swat ungauged: Hydrological budget and crop yield predictions in the upper mississippi river basin. *Transactions of the ASABE* **2010**, *53*, 1533-1546.
39. Vaghefi, S.A.; Mousavi, S.; Abbaspour, K.; Srinivasan, R.; Arnold, J. Integration of hydrologic and water allocation models in basin-scale water resources management considering crop pattern and climate change: Karkheh river basin in iran. *Regional environmental change* **2015**, *15*, 475-484.
40. Evans, R.G. ; Sadler, E.J., Methods and technologies to improve efficiency of water use. Water resources research, 2008, 44(7).
41. Zwart, S.J.; Bastiaanssen, W.G. Review of measured crop water productivity values for irrigated wheat, rice, cotton and maize. *Agricultural water management* **2004**, *69*, 115-133.
42. Molden, D.; Oweis, T.Y.; Steduto, P.; Kijne, J.W.; Hanjra, M.A.; Bindraban, P.S.; Bouman, B.A.M.; Cook, S.J.; Erenstein, O.; Farahani, H. Pathways for increasing agricultural water productivity. In *Water for food water for life: A comprehensive assessment of water management in agriculture*, Taylor and Francis AS: 2007.
43. Naraqi, M.; Akbari, G.A.; Banihabib, M.E. Optimal crop pattern for lake urmia. In *The first international and the fourth national conference of Iran's Environmental and Agricultural Research*, 2015.
44. Labadie, J.W. Modsim: Decision support system for integrated river basin management. **2006**.

45. Azevedo, L.G.T.d.; Gates, T.K.; Fontane, D.G.; Labadie, J.W.; Porto, R.L. Integration of water quantity and quality in strategic river basin planning. *Journal of water resources planning and management* **2000**, *126*, 85-97.
46. Morway, E.D.; Niswonger, R.G.; Triana, E. Toward improved simulation of river operations through integration with a hydrologic model. *Environmental Modelling & Software* **2016**, *82*, 255-274.
47. Emami, F.; Koch, M. Evaluating the water resources and operation of the boukan dam in iran under climate change. *Eur. Water* **2017**, *59*, 17-24.
48. Shourian, M.; Mousavi, S.; Tahershamsi, A. Basin-wide water resources planning by integrating pso algorithm and modsim. *Water resources management* **2008**, *22*, 1347-1366.
49. Bertsekas, D.P.; Tseng, P. Partial proximal minimization algorithms for convex pprogramming. *SIAM Journal on Optimization* **1994**, *4*, 551-572.
50. Kennedy, J.; Eberhart, R. In *Pso optimization*, Proc. IEEE Int. Conf. Neural Networks, 1995; IEEE Service Center, Piscataway, NJ: pp 1941-1948.
51. Kennedy, J. In *The particle swarm: Social adaptation of knowledge*, Evolutionary Computation, 1997., IEEE International Conference on, 1997; IEEE: pp 303-308.
52. Parsopoulos, K.E.; Vrahatis, M.N. Recent approaches to global optimization problems through particle swarm optimization. *Natural Computing* **2002a**, *1*, 235-306.
53. Parsopoulos, K.E.; Vrahatis, M.N. Particle swarm optimization method for constrained optimization problems. *Intelligent Technologies–Theory and Application: New Trends in Intelligent Technologies* **2002b**, *76*, 214-220.
54. Eberhart, R.C.; Shi, Y. In *Comparison between genetic algorithms and particle swarm optimization*, International conference on evolutionary programming, 1998; Springer: pp 611-616.
55. Clerc, M.; Kennedy, J. The particle swarm-explosion, stability, and convergence in a multidimensional complex space. *IEEE transactions on Evolutionary Computation* **2002**, *6*, 58-73.
56. Stewart, J.I.; Robert, M. Functions to predict effects of crop water deficits. **1973**.
57. Steduto, P.; Hsiao, T.C.; Fereres, E.; Raes, D. *Crop yield response to water*. FAO Rome: 2012; Vol. 1028.
58. Alizadeh, A.; Kamali, G. Crops water requirements in iran. *Emam Reza University* **2007**.
59. Arnold, J.; Kiniry, J.; Sirinivasan, R.; Williams, J.; Haney, E.; Neitsh, S. *Swat input–output documentation, version 2012. Texas water resource institute*; TR-439: 2012.
60. Ministry of the Energy. Executive strategies for decreasing 40% of agricultural water demands in zarrine and simineh river basins (saeenghaleh and miandoab areas), volume 7: Studies of water resources and demands planning and management;. *Urmia Lake Restoration Committee, Iran* 2016.